PACIFIC SUBDUCTION COEVAL WITH THE KAROO MANTLE PLUME: THE EARLY JURASSIC SUBCORDILLERAN BELT OF NORTHWESTERN PATAGONIA

C.W. Rapela[1], R.J. Pankhurst[2], C.M. Fanning[3] & F. Hervé[4]

[1]Centro de Investigaciones Geológicas, Calle 1 No. 644, 1900 La Plata, Argentina; crapela@cig.museo.unlp.edu.ar

[2]NERC Isotope Geosciences Laboratory, Keyworth, Nottingham NG12 5GG, UK; r.pankhurst@nigl.nerc.ac.uk

[3]PRISE, Research School of Earth Sciences, The Australian National University, Mills Road, Canberra ACT 0200, Australia; mark.fanning@anu.edu.au

[4]Departamento de Geología, Universidad de Chile, Casilla 13518, Correo 21, Santiago, Chile; fherve@uchile.c

Running Title: Subcordilleran Magmatism of Patagonia

Text words 7,240
References 100
Figures 10
Tables 3

Abstract

The Early Mesozoic magmatism of southwestern Gondwana is reviewed in the light of new U–Pb SHRIMP zircon ages (181 ± 2, 181 ± 3, 185 ± 2, and 182 ± 2 Ma) that establish an Early Jurassic age for the granites of the Subcordilleran plutonic belt in northwestern Argentine Patagonia. New geochemical and isotopic data confirm that this belt represents an early subduction-related magmatic arc along the proto-Pacific margin of Gondwana. Thus subduction was synchronous with the initial phase of Chon Aike rhyolite volcanism ascribed to the thermal effects of the Karoo mantle plume and heralding rifting of this part of the supercontinent. Overall, there is clear evidence that successive episodes of calc-alkaline arc magmatism from Late Triassic times until establishment of the Andean Patagonian Batholith in the Late Jurassic involved westerly migration and clockwise rotation of the arc. This indicates a changing geodynamic regime during Gondwana break-up and suggests differential roll-back of the subducted slab, with accretion of new crustal material and/or asymmetrical ‘scissor-like’ opening of back-arc basins. This almost certainly entailed dextral displacement of continental domains in Patagonia, and is not easily reconciled with the possible overlap of the Antarctic Peninsula to the west in Jurassic reconstructions.

The causal links between subduction-related magmatism, mantle plumes and Gondwana break-up during Jurassic-Late Cretaceous time is a major issue in Earth history (e.g., Storey 1995). Ultimate answers to many questions on this topic may only come from studies of mantle dynamics, but precise geochronological, geochemical and isotope studies can provide important constraints to models of supercontinent break-up.

Patagonia, in southernmost South America, is a key area in the break-up history of SW Gondwana as it preserves the largest acid magmatic province developed during rifting (the Chon Aike province, Pankhurst *et al.* 1998 and references therein) and, subsequently, protracted subduction-related magmatism on the Pacific margin (Fig. 1). Together, these provide a complete magmatic record of pre-, syn-, and post-break up episodes. The timing and characteristics of the Early Cretaceous stage of supercontinent break-up that culminated with the eruption of the Paraná–Etendeka flood basalts and the opening of the South Atlantic is well known (Turner *et al.* 1994 and references therein), whereas the geodynamic environment in the proto-Pacific margin of SW Gondwana during initial rifting in the Early Jurassic (~ 180 Ma; Storey 1995) is still poorly understood.

In this paper we present new U-Pb SHRIMP data for the emplacement of Early Jurassic granitic rocks in the Subcordilleran belt of northwestern Patagonia (Fig. 1). Their crystallization ages are used, together with geochemical and Sr-Nd isotopic data to investigate the generation, spatial distribution and migration with time of I-type magmatism in Patagonia, from Late Triassic to Cretaceous times. The significance of this magmatic history is reviewed in terms of a possible palaeogeographical reconstruction of southwestern Gondwana and other break-up magmatism including the Jurassic rhyolites of Patagonia and the Karoo–Ferrar basaltic provinces.

Late Triassic to Jurassic Igneous Episodes in Patagonia

Batholith of Central Patagonia and Deseado Monzonite Suite

The Late Triassic ‘Batholith of Central Patagonia’ (Fig. 1), represents the culmination of I-type granite magmatism that started in Permian times across the North Patagonian Massif (Pankhurst *et al.* 1992; Rapela *et al.* 1992). Departing from the typical N–S Andean alignment, the Batholith of

Central Patagonia is associated with a NW–SE fault system that extends from Lago Panguipulli in Chile to the Gastre area in central Patagonia. Rapela (2001) reviewed its lithology, geochemistry and isotopic characteristics. Its known chronology is based on Rb-Sr isochrons defined in the Gastre area, indicating two separate episodes in the Late Triassic (Gastre Superunit 220 ± 3 Ma and Lipetrén Superunit 208 ± 1 Ma, Rapela *et al.* 1992). The Triassic age of the Gastre superunit is now supported by the authors' unpublished U–Pb zircon age of 221 ± 2 Ma. Satellite plutons are located to the north of the batholith, in the North Patagonian Massif (Rb-Sr isochrons of 210 ± 2 Ma and 210 ± 9 Ma, Cingolani *et al.* 1991; Rapela *et al.* 1996). The volcanic counterparts of these Late Triassic plutonic rocks are calc-alkaline rhyolitic ignimbrites interbedded with air-fall deposits carrying a rich *Dicroidium* and associated flora (Rb-Sr isochron of 222 ± 2 Ma, Rapela *et al.* 1996). Finally, the southernmost granitic outcrops correlated with the Batholith of Central Patagonia belong to the Deseado Monzonite Suite, located in the north-eastern sector of the Deseado Massif (Fig. 1). These rocks are characterized by the abundance of quartz monzodiorite and quartz monzonite (Godeas 1993; Rapela & Pankhurst 1996), and have been dated as earliest Jurassic by precise Rb-Sr isochrons, at 202 ± 2 Ma and 203 ± 2 Ma (Pankhurst *et al.* 1993).

Chon Aike province

The Chon Aike province is one of the largest rhyolitic provinces in the world (Fig. 1) and also partly extends to the Antarctic Peninsula. Silicic eruptions started with an Early Jurassic episode in northeast Patagonia migrated to southern Patagonia in Middle Jurassic time and finally moved to the Andean cordillera during the Late Jurassic (Féraud *et al.* 1999; Pankhurst *et al.* 2000 and references therein). Pankhurst *et al.* (2000) identified these three phases as V_1 (188–178 Ma), V_2 (172–162 Ma), and V_3 (157–153 Ma); their precise definitions are subject to modification as new data become available – for example, Pankhurst *et al.* (2003a) have reported U–Pb zircon ages of 138 ± 2 Ma (i.e., Early Cretaceous) for rhyolites in Chile that are traditionally correlated with the V_3 group in Argentina. In this paper we retain these ranges, slightly extended to allow for analytical errors in the published age determinations.

The Early and Middle Jurassic pulses do not have coeval cordilleran counterparts in the main body of the Patagonian batholith, and have been ascribed to crustal melting due to spreading of the Karoo plume head (Pankhurst *et al.* 2000; Riley *et al.* 2001). The Middle and Late Jurassic pulses show the geochemical influences of an active margin (Riley *et al.* 2001), and the youngest pulse of Chon Aike rhyolite volcanism (V_3) starts before, but partially overlaps in age, the earliest units of the southern Patagonian batholith.

Subcordilleran belt

The Subcordilleran belt (SCB) of Río Negro and Chubut provinces is a discontinuous belt of Early Jurassic igneous rocks and Liassic sediments, that extends for more than 250 km immediately to the east of North Patagonian cordillera (Figs 1, 2). The NNW–SSW elongated basin is delimited by a dominantly deltaic and tidal marine facies of Liassic black shales, siltstones, conglomerates, quartz-feldspar sandstones and limestones, with volcanic and volcaniclastic intercalations (Lizuaín 1999 and references therein). Because of the contemporaneous volcanism (and local intrusion by gabbroic bodies), this basin was assigned an intra-arc setting by Page & Page (1999). The littoral deposits of the basin are abnormally thick for a transgressive succession, suggesting development of coastal cliffs and shorelines undergoing tectonic uplift (González Bonorino 1990). Black mudstones, siltstones and volcaniclastic rocks are found in deep boreholes through the San Jorge basin at *ca.* 46ºS; 69º 30´W, and are the southernmost reported occurrence of the Liassic marine sediments (Uliana & Legarreta 1999).

The plutonic rocks of the SCB were called ‘Subcordilleran Patagonian Batholith’ by Gordon & Ort (1993), and renamed the ‘Subcordilleran Plutonic Belt’ by Haller *et al.* (1999) on the grounds that a single continuous body is not seen. Subalkaline norite and olivine gabbro are abundant in the sierras of Tepuel and Tecka in the southern part of the belt (Page & Page 1999; Fig. 2). In the northern part of the belt, granitic and gabbroic plutons are intruded into foliated granites and metamorphic rocks of Palaeozoic age, while in the southern sector they were intruded or tectonically emplaced in Carboniferous sediments of the Tepuel basin or the Liassic sediments of the SCB. The gabbros are intruded in turn by Cretaceous satellite plutons of the Patagonian

batholith (Page & Page 1999). The granitic rocks of the SCB are zoned plutons dominated by I-type biotite-hornblende granodiorite and quartz monzodiorite, and biotite monzogranite, with minor diorite and leucogranite (Spikermann *et al.* 1988, 1989; Gordon & Ort 1993; Busteros *et al.* 1993; Haller *et al.* 1999).

Previous studies and sampling.

The Alto Río Chubut area was studied by Gordon & Ort (1993) who recognized two main units: the Arroyo La Tuerta granodiorite dominated by hornblende-biotite granodiorites and tonalites with abundant mafic enclaves and syn-plutonic dykes, and the La Angostura granite composed of biotite monzogranites and granodiorites with occasional hornblende. Minor gabbro bodies also occur associated with the granites. Based on field relationships the main units were interpreted as coeval and comagmatic, defining a zoned-type intrusion, with Rb–Sr isochron ages of 200 ± 24 Ma for the Arroyo La Tuerta granodiorite and 183 ± 13 Ma for La Angostura granite (Gordon & Ort 1993). The Leleque area was studied by Lizuaín (1983) and Gordon & Ort (1993), who recognized two units: a small gabbro pluton, and a dominant hornblende-biotite granodioritic to monzogranitic phase cutting the gabbro. The modal compositions of the granites in the Leleque and Alto Río Chubut areas are indistinguishable (Rapela 2001). A K–Ar age of 141 ± 5 Ma was reported for the Leleque unit by Lizuaín (1983), while K–Ar ages of 177 ± 5 and 173 ± 10 Ma were obtained in diorites and tonalites at the northern margin of Lago Puelo near the Leleque area (Lizuaín 1981). Sample SER-046 (41°58'04.4"S;71°16'13.7"W) is a weathered biotite monzogranite from La Angostura granite in the southern sector of the Alto Río Chubut area, whereas LEL-052 (42º21'22.6"S; 71º11'10.7"W) is a hornblende-biotite (hornblende-biotite) granodiorite from the dominant suite at Leleque, which carries microgranular mafic enclaves of 6–15 cm.

The Aleusco batholith in the Precordillera of Chubut was first described by Turner (1982) and Spikermann *et al.* (1988, 1989). Spikermann *et al.* (1988) and Haller *et al.* (1999) reported K–Ar ages of 180 ± 10 Ma, and 177 ± 6 Ma, 179 ± 7 Ma and 184 ± 6 Ma respectively. The Aleusco body is a composite epizonal pluton emplaced in Liassic sediments. It consists of a main facies of hornblende-biotite granodiorite and subordinate diorite with abundant mafic enclaves, and late

plutonic leucogranite and aplite. Sample ALE-055 (43º06'14.6"S; 70º28'39.7"W) is a typical hornblende-biotite granodiorite of the main facies (Fig. 3).

Near the locality of José de San Martin in Chubut province, a string of NE-SW granitic bodies, mainly emplaced into Carboniferous and Liassic sediments, are the southernmost outcrops of the SCB. The petrology and chemical characteristics of these granitoids have been described by Spikermann (1978), Franchi & Page (1980) and Busteros *et al.* (1993). Franchi & Page (1980) reported K–Ar ages of 167 ± 30 Ma, 197 ± 10 Ma and 207 ± 10 Ma for these rocks, which they referred to as the José de San Martín Formation. The dominant lithology is medium-K metaluminous granodiorite varying to monzodiorite. The largest exposure is a 10 km-long, 2 km-wide pluton with a thermal aureole in Upper Palaeozoic sediments, 6 km to the east of the town of José de San Martín. Sample JSM-058 (44º00'27.5"S; 70º23'39.6"W) is a hornblende-biotite quartz monzodiorite when classified by modal proportions, and a tonalite in the normative Ab-An-Or diagram (Fig. 3).

The abundant subalkaline gabbros of the southern sector of the SCB (Fig. 2) are recognized as a separate lithostratigraphic unit, the Tecka Formation, which is dominated by norite and olivine gabbro, with minor anorthosite, peridotite and troctolite (Page & Page 1999). An ^{40}Ar–^{36}Ar age of 182.7 ± 1 Ma has been reported for a gabbro of the Tecka Formation (Féraud *et al.* unpublished data cited by Page & Page 1999), while a U–Pb SHRIMP age of 191 ± 3 Ma was obtained within a complex zircon population with Precambrian inheritance in an Opx-Cpx gabbro on the southern shore of Lago Fontana (Muzzio gabbro, Rolando et al. 2002). Two samples were collected from the Tecka Formation, a Cpx-Opx quartz gabbro near Quichaura (QUI-225; 43º31'30.9"S; 70º39'34.4"W) and an Ol-Cpx-Opx gabbro west of Gualjaina (QUI-227; 42º45'01.9"S; 70º48'43.9"W), as well as a sample of Cpx-Opx quartz gabbro from the Muzzio gabbro on the southern shore of Lago Fontana (MUZ-224; 44º58'23.4"S; 71º28'10.0"W).

U–Pb Geochronology

U–Pb dating was carried out using sensitive high-resolution ion microprobes (SHRIMP RG and SHRIMP II) at The Australian National University, Canberra, following the procedures of

Williams (1998). Cathodo-luminescence images show that all the zircons are relatively simple with concentric zonation of the outer parts of the grains and no obviously inherited cores (Fig. 4). Analysis targets were mostly within the well-zoned rims and tips of euhedral grains, and were selected so as to avoid cracks and inclusions. Data for the SHRIMP analyses were processed using SQUID (Ludwig 2001) and Isoplot/Ex (Ludwig 1999), and ages were calculated from the $^{206}Pb/^{238}U$ ratios corrected for the appropriate composition of common Pb based on the measured ^{207}Pb (Table 1).

Tera-Wasserburg diagrams (Fig. 5) show results for the analysed samples described above from La Angostura, Leleque, Aleusco and José de San Martín. Seventeen grains from the granite at La Angostura were analysed and gave a mean age of 181 ± 2 Ma (MSWD = 2.0). Nineteen grains were analysed from the Leleque granodiorite, of which one is clearly inherited (c. 330 Ma). Even discounting this, the data spread outside expected analytical error (MSWD = 3.2), and the four youngest $^{206}Pb/^{238}U$ ages were disregarded as probably suffering from slight Pb-loss, apparently at about 174 Ma (perhaps as a result of V_2 volcanic heating). The remaining 14 define an Early Jurassic age of 181 ± 3 Ma. From the 14 analysed grains from the Aleusco granodiorite, one suffered from an unusually high analytical uncertainty and one appears to have suffered Pb-loss as in LEL-052; the remaining 12 grains define an Early Jurassic age of 185 ± 2 Ma. Finally, 12 grains of a quartz monzodiorite from the José de San Martín body also gave a Early Jurassic age of 182 ± 2 Ma, discounting three grains in which Pb-loss is apparent.

Geochemistry

The U–Pb results clearly demonstrate that the granites of the SCB are of Early Jurassic age, essentially contemporaneous with the V_1 episode of rhyolite volcanism in the North Patagonian Massif (188–178 Ma). Their geochemistry will be considered in the overall context of Late Triassic to Early Jurassic magmatism in the region and the subsequent plutonism of the Andean Patagonian batholith, an archetypical example of a continental margin subduction-related granite batholith (Fig. 1). The geochemical database consists of 35 samples of the Subcordilleran belt (including the 3 granites and 3 gabbros from Table 2), and equivalent numbers from the other units (see figure

captions for sources). The major element compositions of most of the plutonic rocks show general similarities in the normative An-Ab-Or diagram (Fig. 3). The Batholith of Central Patagonia and the Deseado monzonite suite lack the conspicuous An-rich facies (typically gabbros and diorites) typical of the Late Jurassic to Pliocene Patagonian batholith, but the association with basic plutonic rocks in the SCB suggests a very close affinity with the Patagonian batholith. The abundance of gabbros and basic rocks in the SCB (assuming the Tecka Formation gabbros to be coeval with the granites), is most probably underestimated in Fig. 3, as they form conspicuous outcrops in the southern part of the belt.

The sample from La Angostura (SER-046) was considered too weathered for whole-rock analysis, but published data for this area are included in the geochemical plots. New chemical analyses of granitic rocks from the main facies in the Leleque, Aleusco and José de San Martín areas as well as representative samples of the abundant gabbros from the southern part of the belt are shown in Table 2. The granitic rocks are all subalkaline metaluminous granodiorite/tonalites/ monzogranites with an ASI = 0.91–0.96 (ASI: Alumina Saturation Index = molecular $Al_2O_3/CaO+Na_2O+K_2O$), SiO_2 61.46–69.66%, Na_2O+K_2O 6.01–7.28%, FeOt+MgO 3.58–8.25%, REE patterns with $[La/Yb]_N$ = 4.7–10.5 and a weak negative Eu anomaly (Eu/Eu* = 0.67–0.78) (Table 2, Figs 6, 7b). The overall subalkaline geochemistry of these granites is typically that of I-type granites produced by melting of igneous sources (Chappell & White 1992). Furthermore, the Ga/Al (1000*Ga/Al = 2.2), Rb/Zr (0.5–0.7) and FeOt /MgO (2.4–2.9), Zr/Nb (>17) and Ba/La (~ 20) ratios are characteristic of metaluminous magmas emplaced in convergent margins rather than intraplate settings (Pearce *et al.* 1984; Whalen *et al.* 1987; Eby 1990). Major and trace element Harker and multi-element diagrams show that data for the granitic rocks of the SCB all plot within the fields defined by a large geochemical data set for the Patagonian batholith (Figs 6, 7a). The main facies of the different granitic complexes of the SCB show enrichment of Rb, Ba and Th relative to Nb, Ta, REE, Hf and Zr (Fig. 7a), a characteristic of magmatic arc rocks (Thompson *et al.* 1984). More specifically, they show the same patterns as the hornblende-biotite granodiorites and tonalites of the Patagonian batholith.

The arc geochemical signature of the granitic rocks is shared by the abundant subalkaline gabbros of the southern part of SCB, which show arc-tholeiite affinities when normalized against MORB (Fig. 7b), and are inferred to be subduction-related basic rocks (Page & Page 1999). Remarkably, the shape of the MORB-normalized patterns of the basic rocks mimic those of the granites, but the latter are more enriched in highly incompatible elements (Fig. 7b). The plagioclase-rich olivine gabbro QUI-227 has a REE pattern with a positive Eu anomaly (Fig. 7c), suggesting that some of the basic rocks are cumulate-rich facies, consistent with the widespread cumulate fabric of the association and the occurrence of minor anorthosites and ultrabasic bodies reported by Page & Page (1999). It is therefore possible that the granitic rocks of the SCB were derived by fractional crystallization from the basic coeval magmas, at least in part. The gabbros from the Quichaura and Muzzio bodies (QUI-225 and MUZ-224) are indistinguishable in all geochemical respects, demonstrating without doubt that the later is a member of the Tecka Formation, and that the Subcordilleran plutonic belt extends over at least 300 km from La Angostura to Lago Fontana.

Compared to the SCB granites, the dominant facies of the Late Triassic Batholith of Central Patagonia and the Deseado Monzonite Suite (62–68% SiO_2) are enriched in P_2O_5 and Sr, with relatively high Sr/Y ratios and low FeOt /MgO ratios (Fig. 6).

None of the Triassic and Jurassic plutonic rocks of Patagonia have geochemical characteristics of the TTD (trondhjemite-tonalite-dacite) “adakite” suite, formed by partial melting of subducted ocean crust according to Drummond *et al.* (1996). Such compositions are recognized in Andean Miocene–Holocene dacites at 48º–54ºS (Kay *et al.* 1993; Stern & Kilian 1996), and *c.* 70 Ma-old trondhjemites at 53ºS in the Patagonian batholith (Bruce 1988). The Deseado monzonite suite shows some geochemical affinities with the TTD association, such as a tendency to high Sr/Y (Fig. 6) and depletion of HREE, but high LIL (large-ion lithophile) element concentrations and enriched Sr and Nd isotopic signature rule out a depleted N-MORB source (Rapela & Pankhurst 1996).

The Early Jurassic V_1 group of silicic volcanic rocks, which crop out in Patagonia east of the Andes and at the same latitudes as the SCB (Fig. 1), show geochemical signatures very different

from the majority of the I-type granites. These high-K rhyolites and ignimbrites are enriched in alkalis, P_2O_5, and notably in Zr and Nb, notably in the intermediate SiO_2 range (Fig. 6). In some cases, such as on the Atlantic coast at 45ºS (Península Camarones), they reach peralkaline compositions with high Zr (425–600 ppm, Fig. 6) and TiO_2 (0.45–0.95%) (Pankhurst & Rapela 1995). Coeval V_1 rhyolites in the Antarctic Peninsula show similar geochemical characteristics to those of Patagonia (Riley *et al.* 2001). However, in northern Patagonia, the V_1 group was preceded by the Late Triassic hornblende-biotite ignimbrite of Los Menucos, which shows geochemical trends akin to those of the contemporaneous I-type units of the Batholith of Central Patagonia (Fig. 6).

The easternmost rhyolites and ignimbrites of the Middle Jurassic V_2 group, located near the Atlantic coast at 47º45´S (Puerto Deseado), are also enriched in Nb and Zr (Fig. 6). In contrast, the remainder of the V_2 group and the younger Middle-Late Jurassic V_3 group, located in Andean and pre-Andean regions, exhibit major and trace element abundances and trends similar to those observed in the I-type granites (Fig. 6). It is worth noting that Riley *et al.* (2001) concluded that all three rhyolite groups inherited some subduction-related trace element characteristics from their source, although less so in V_1 than in V_2 and V_3.

Nd and Sr Isotope Data

Nd and Sr isotope ratios were determined on four SCB granite samples (Table 3). In Fig. 8 their initial isotope compositions are compared with those of other Mesozoic–Cenozoic I-type granites, and the extensive Triassic and Jurassic volcanic rocks of Patagonia for which precise U–Pb, Ar–Ar and Rb–Sr dating have been reported (Pankhurst & Rapela 1995; Feraud *et al.* 1999; Pankhurst *et al.* 2000).

Data for the SCB granites mostly plot within the field of the Late Jurassic–Miocene I-type granites of the Patagonian batholith, as do those of the Deseado monzonite suite and the Batholith of Central Patagonia (Fig. 8a). Samples LEL-052 and ALE-055 have εNdt values indistinguishable from those of the Deseado suite, which range from -0.3 to -2.5. The quartz monzodiorite of José de San Martín (JSM-058) is the most primitive of all the Jurassic and Triassic I-type granites, with a

depleted-mantle signature comparable to that of Mid-Cretaceous granites in the Patagonian batholith (Pankhurst *et al.* 1999). A microdiorite enclave in the monzodiorite (JSM-059) gives the same Nd and Sr isotopic signature, confirming the same primitive source. Late Jurassic tonalites, granodiorites and quartz monzodiorites of *c*. 150 Ma that can be considered the earliest event of the Patagonian batholith (Martin *et al.* 2001; Pankhurst *et al.* 2000; Suárez & De la Cruz 2001) plot in the enriched-source sector of the Nd–Sr isotopic diagram. Data for Late Jurassic satellite bodies located east of the batholith, such as the Sobral tonalite (Pankhurst *et al.* 2000; Fig. 8a), confirm that, the earliest magma batches of I-type magmas are among the most isotopically-evolved of the batholith, regardless of geographical location. In contrast, the Sm–Nd relationships of granitoids from the Patagonian batholith at 44º–46ºS indicate source compositions that change from slightly LIL-enriched for the Early Cretaceous rocks to significantly depleted for the Early Miocene rocks, the latter in turn very similar to those of the Tertiary to Recent mafic strato-volcanoes of the Southern Volcanic Zone of the Andes (Pankhurst *et al.* 1999). Bruce *et al.* (1991) also showed a broad regional trend of decreasing initial $^{87}Sr/^{86}Sr$ with time, with some values as high as 0.707 for Late Jurassic–Early Cretaceous granites at 48ºS.

None of the extensive Triassic and Jurassic volcanic rocks of Patagonia seem to be derived from long-term LIL-depleted sources such as those of the SCB granites and the Mid Cretaceous–Tertiary granites of the Patagonian batholith (Fig. 8b). In particular, many of the earliest rhyolitic rocks of northern Patagonia have εNdt values that fall significantly below the field of I-type batholiths, with low εNdt at relatively low $^{87}Sr/^{86}Sr$ (Fig. 8b). In the case of the V_1 group rhyolites, this signature has been ascribed to a hypothetical Grenville-age lower crust (Pankhurst & Rapela 1995; Riley *et al.* 2001), implying a completely different genesis to that of the coevally emplaced granites of the SCB. However, some Early Cretaceous granites of the Patagonian batholith plot on a steep trend extending towards the compositions of these V_1 rhyolites, suggesting contamination of mantle-derived magmas with lower crustal melts (Pankhurst *et al.* 1999).

Simple mixing arrays between melts derived from the lithospheric mantle wedge and either upper or lower crustal contaminants could explain the isotopic trends observed in I-type granites

(Fig. 8c). The change towards depleted-source melts with time in the Patagonian batholith has been attributed to a progressive decrease in crustal contamination due to 'magmatic inflation' during the growth of the body, whereby younger magmas emplaced along the axis of the batholith were physically isolated from contamination by radiogenic wall rocks by earlier intrusions (Bruce *et al.* 1991). However, if the isotopic composition of the main source of all I-type magmas were always similar to (or more primitive than) that of the Tertiary granites (εNdt values between -4 and –6, Pankhurst *et al.* 1999), it is difficult to understand why depleted signatures are *never* observed in Triassic and Jurassic granites nor any of the Andean volcanic rocks (V_3 Group, Fig. 8b). Instead, we suggest that melting occurs in progressively more LIL-depleted sources with time and that the relatively primitive signature of the abundant Mid Cretaceous–Tertiary granites is indicative of melting in the lithospheric mantle underlying the Patagonian batholith (Fig. 8c). The evolved composition of Late Triassic to Early Cretaceous granites could then be explained by variable amounts of upper and lower crustal contamination of melts derived from an effectively undepleted lithospheric source, such as that represented by the Deseado monzonite suite or the granites of the SCB (Fig. 8a,c).

The Subcordilleran belt: remnant of an Early Jurassic magmatic arc

The U-Pb SHRIMP crystallization ages of typical metaluminous granodiorites and quartz monzodiorites from the SCB between 42º and 44º S are remarkably consistent, much more precise than the Rb–Sr and K–Ar ages reported for similar rocks by Gordon & Ort (1993) and Haller *et al.* (1999), and compatible with the Ar–Ar age for the subalkaline gabbros given by Page & Page (1999). The age interval of 187–178 Ma allowing for analytical error, falls in the Pliensbachian and Toarcian stages of the GSA and IUGS-ISC time-scales (Palmer & Geissman 1999; Remane *et al.* 2000). Altogether the data presented here for four separate granite bodies in the Subcordilleran belt indicate that I-type magmatism of short apparent duration was emplaced into the 300 km long (at least) Liassic sedimentary basin within a very few million years of its deposition. It cannot be traced south of 44º30'S, although Early Jurassic arc rocks could be buried by Cretaceous sediments in the San Jorge basin or by thick Middle Jurassic ignimbrites and Tertiary plateau basalts in the

Deseado Massif. The 700 m thick sequence of fossil-bearing Liassic marine sediments and volcaniclastic rocks found in deep boreholes of the San Jorge basin at 46ºS (Uliana & Legarreta 1999), suggest that this possibility would be worth testing in future research. Nevertheless, the timing and disposition of SCB magmatism show that this was a distinct event from both the Triassic 'oblique' batholiths and the Patagonian batholith (Fig. 9). Early Jurassic ages have not been reported from any part of the Patagonian batholith.

On the other hand, the geochemistry and isotopic signature of the SCB I-type granites and coeval basic rocks are typical of subduction-related cordilleran-type belts in convergent continental margins, and cannot be distinguished from those of the Andean batholiths emplaced in the Pacific margin of South America after Gondwana break-up (Figs 3,6-8). Furthermore, emplacement in a continental-margin marine basin, filled with littoral sediments and coeval volcanic and volcaniclastic rocks, suggests an intra-arc environment (Lizuaín 1999; Page & Page 1999).

I-type magmatism, rhyolite provinces and Gondwana break-up

The I-type batholiths and plutons of Patagonia record a complex Mesozoic history of convergence episodes that preceded, were coeval with, and outlasted the major stages of supercontinent rifting. The relative abundance of mafic igneous rocks in the SCB and the Patagonian batholith, associated the final stage of rifting and the active opening of the South Atlantic ocean, is perhaps the most important lithological difference from the Triassic I-type suites emplaced during early supercontinental convergence and rifting.

The geometrical relationships between the Karoo-Ferrar provinces, the proto-Pacific subduction margin and the supercontinent break-up lines (Fig. 10) suggest that these are all inter-related and that Karoo magmatism initiated separation between Eastern and Western Gondwana (Cox 1992, and references therein). The data presented here for the SCB granites demonstrates that initiation of Andean-type subduction in Patagonia was coincident with intraplate magmatism, including the mafic magmatism of the Ferrar and Karoo mafic igneous provinces at 184–179 Ma, with a climax at 183 Ma (Encarnación *et al.* 1996; Duncan *et al.* 1997;), and the contemporaneous V_1 episode of rhyolitic magmatism in northeastern Patagonia (Fig. 9). Recently, Riley et al. (2004) have shown,

also using SHRIMP U–Pb zircon dating, have shown that Karoo rhyolites in the Lebombo area of eastern South Africa were erupted between 182 ± 3 and 180 ± 2 Ma, indistinguishable from the age of the SCB granites. Thus, although Elliot & Fleming (2000) argued for a single source for the mafic lavas, centred on a triple junction in the proto-Weddell Sea, felsic magmatism associated with this event extended far away from the site of the Karoo plume, reaching the proto-Pacific margin of the supercontinent, as suggested by Pankhurst *et al.* (2000).

Middle Jurassic magmatic activity shifted towards southern Patagonia and the Antarctic Peninsula, developing the extensive rhyolites sequences of the Chon Aike Formation (V_2 event, Pankhurst *et al.* 2000) (Figs 1, 9). In Tierra del Fuego, the peraluminous Darwin granite suite is thought to be a correlative of the V_2 rhyolites (164.1 ± 1.7 Ma, Mukasa & Dalziel 1996). This Middle Jurassic acid event (~172–162 Ma: εNdt = -1.8 to -3.9; initial $^{87}Sr/^{86}Sr$ = 0.7064–0.7169) is now the only one for which no I-type cordilleran counterpart has been reported (Fig. 9), although further systematic and precise geochronological work will be necessary to confirm such a temporal hiatus in the subduction-related cordilleran magmatism along the southern and austral Andes.

From Late Jurassic to Tertiary times, the main locus of I-type magmatic activity defines the axis of the modern Andean Cordillera (Rapela & Kay 1988). The plutonic component of this activity is represented by the Patagonian batholith, which ranges in age from *c.* 155 to 5 Ma. The oldest granites (155–143 Ma, Late Jurassic) are restricted to the eastern side of the batholith and satellite plutons east of the Patagonian batholith (Bruce *et al.* 1991; Martin *et al.* 2001; Suarez & De la Cruz 2001, Rolando *et al.* 2002). Late Jurassic K-Ar ages have also been reported from the northeastern sector of the Patagonian batholith (39º 42´-42ºS) (González Díaz 1982; Rapela & Kay 1988) whereas ages in this range have not been identified along the western side of the batholith. Late Jurassic volcanic rocks also occur along the length of the Patagonian Andes, as well as in Argentine sectors of the North Patagonian and Deseado massifs (Pankhurst *et al.* 2000; Suarez & De la Cruz 2001 and references therein). Thick rhyolite sequences of the V_3 group (~ 157–153 Ma and younger) in the Andean sector of southern Patagonia are considered to be active-margin volcanic products associated with the Late Jurassic granites (Pankhurst *et al.* 2000). On the oceanic

side of the Andes, this volcanism continued locally into Cretaceous times (e.g., Suárez & De la Cruz 1997a,b; Pankhurst *et al.* 2003a).

From the above described space-time relationships of the I-type belts it is clear that during the Early Jurassic to Early Cretaceous time interval there was a significant ocean-ward migration of the magmatic arc (of at least 150 km at the latitude of José de San Martín, Fig. 1). In the northern Antarctic Peninsula and Thurston Island (Fig. 10), Jurassic subduction-related magmatism also migrated from the eastern margin towards the western margin, with emplacement of granitic plutons closer to the trench (Pankhurst 1982). Thus ocean-ward migration of the arc during the Jurassic was probably a continental scale characteristic of the proto-Pacific margin of southwestern Gondwana. This westward shift of the cordilleran I-type belts ceased after the opening of the South Atlantic, the distribution of the Early Cretaceous to Miocene plutons of the Patagonian batholith suggesting a quasi-stationary position.

However, the NNW-SSE orientation of the SCB compared with the N-S trend of the North Patagonian cordillera (Fig. 1) suggests that the ocean-ward shift of the arc could be better described as a clockwise migration of the axis in northern Patagonia. The regular decrease of Ar–Ar ages in the rhyolites of Patagonia from the ENE (~ 187 Ma) to the WSW (~ 144 Ma) along about 650 km (Féraud *et al.* 1999) might be also explained by back-arc crustal extension behind a clockwise migrating arc. Palinspastic restoration of the Patagonian orocline at 56º S shows the opening of a 230 km wide oceanic back-arc basin at this latitude, also indicating Early–Mid Jurassic to Early Cretaceous clockwise rotation of the magmatic arc (Dalziel 1981; Kraemer 2003 and references therein), a conclusion remarkably coherent with the results of this study. The NW-SE strike of the Batholith of Central Patagonia (Fig. 1) could also be taken as suggesting that migration of the magmatic arc may have started during the Late Triassic (Fig. 10), although the present spatial relationships could be, at least in part, an artifact resulting from crustal extension and block displacements away from the Karoo mantle plume (Fig. 10). In any case, the development of the SCB during the Early Jurassic involved an important re-arrangement in the geometry of plate convergence in Patagonia, that evolved from oblique belts dominated by intermediate and acid

units that characterized the later Gondwana stage, towards the north-south Andean style, with abundant basic rocks.

Early Jurassic palaeogeography and tectonics

The apparent clockwise rotation with time of the magmatic axis represented by the progression of the elongated Batholith of Central Patagonia, the Subcordilleran plutonic belt, and the Andean Patagonian Batholith, from Late Triassic to Mid Jurassic, is a major geological feature whose causes are not yet well understood. Assuming that they were all formed parallel to, and at a certain distance from, the trench in an active subducting margin, they suggest that the margin of southwest Gondwana was displaced in the same way during this period.

Major tectonic factors that could be related to such a rearrangement of the margin include:

1. Differential roll-back of the subduction zone, greater in E–W amplitude towards the south. This could have occurred episodically, as there are lulls in plutonic activity, or at least periods without magma-generating subduction, between that of the three batholiths. The 'space' left by the trench stepping out in this way would be filled by accreted or displaced material or by intracontinental extension.
2. Asymmetric ('scissor-like') extension of the Patagonia continental crust increasing to the South. Generation of the Jurassic acid volcanic province in Patagonia suggests a generally extensional environment. Immediately east of the cordillera, the Jurassic Rocas Verdes basin developed as a marginal basin with quasi-oceanic floor and a parautochthonous terrane to the west (with continental crust topped by a magmatic arc) (Dalziel 1981 and references therein), and closed back in a more westerly position in Cretaceous times (Kraemer 2003 and references therein). The existence of a second marginal basin, today represented by the middle Jurassic mafic blueschists of the Diego de Almagro Complex (Hervé and Fanning, 2003) could further enhance this mechanism.
3. Accretion of tectonostratigraphic terranes along the southern part of the margin, resulting in the subduction zone jumping progressively westwards. The Madre de Dios

accretionary complex (Fig. 10) has been considered as exotic to the Patagonian margin (Forsythe 1982), but palaeontological evidence (Ling *et al.* 1987) and detrital zircon dating (Hervé *et al.* 2003) show that the rocks of this complex are mostly of Permian age and that sandstones in the upper part (Duque de York complex) are probably derived from the same cratonic sources as the Eastern Andes Metamorphic Complex, so that accretion must have occurred before rotation of the magmatic axis. The Chonos accretionary complex, like the Trinity Peninsula and LeMay groups of the Antarctic Peninsula (Fig. 10), contain both Permian and Triassic detrital zircons (Hervé *et al.* 2003; I.L. Millar & R.J. Pankhurst, unpublished data), but their times of accretion are not well constrained. It should be noted that continuous development of an accretionary prism, growing from E to W across Patagonia (e.g., Forsythe 1981), would conflict with the proposition that Patagonia has a Grenville-age deep crust (Pankhurst *et al.* 1994).

4. Displacement of terranes along the continental margin during the periods without magmatic activity could also occur by strike-slip continental margin conditions. Left lateral strike slip movement of blocks along the southwestern margin of Gondwana-South America have been well identified for post-Early Cretaceous times (Rapalini *et al.* 2001; Olivares *et al.* 2003), are still active along the Magellan Fault, and may have been also active before. In the Chonos region, the northward late Cenozoic movement of the Chiloé block allowed the formation of the extensional Traiguén basin in a period of trench parallel subduction with no contemporaneous arc magmatism (Hervé *et al.* 1993). Subduction-related magmatism resumed when subduction again became orthogonal (Pankhurst *et al.* 1999).

Prior to development of the Cretaceous arc, the spatial distribution of the highly oblique Late Triassic Batholith of Central Patagonia and the rather less oblique SCB (Fig. 1) is difficult to explain by convergence of the Pacific and the South American plates, differing radically from that prevailing after western Gondwana break-up in Early Cretaceous times. Early Triassic arc magmatism does not continue to the south of the North Patagonian Massif, and explanation of this absence is a major challenge in understanding the evolution of Patagonia. Several factors suggest

that the southern sector of the South American plate is a collage of continental blocks, some of them with strong geological and paleontological affinities with southern Africa. Thus palaeomagnetic and geological studies in the Falkland/Malvinas islands support a 180º tectonic rotation from a pre-Gondwana break-up position adjacent to the southeast coast of South Africa (Mitchell *et al.* 1986; Taylor & Shaw 1989; Marshall 1994; Curtis & Hyam 1998). An original position of part of Patagonia close to southern Africa is also consistent with the remarkable affinities of the Permian and Triassic flora of the Deseado Massif to that of the Karoo basin (Archangelsky 1990; Artabe *et al.* 2003). In addition, the recovery of Cambrian granodioritic orthogneiss from borehole drilling in Tierra del Fuego (Söllner *et al.* 2000; Pankhurst *et al.* 2003b) suggests that the basement of the southern tip of South America may have also been a displaced terrane originally associated with the Cambrian proto-Pacific margin, and also represented by the Cape Granite suite in South Africa and the Ellsworth Mountain in Antarctica (Rapela *et al.* 2003 and references therein) (Fig. 10).

In order to explain the displacement of the Falkland/Malvinas microplate, the oblique spatial arrangement of the Late Triassic magmatism and the 'excess space' problem in the reconstruction of the South Atlantic, Rapela & Pankhurst (1992) proposed the dextral displacement of a southern Patagonian block along the transcontinental Gastre Fault System (Fig. 1). Mafic dykes in the Falkland/Malvinas islands are coeval with (K-Ar and Ar-Ar ages of 180-192 Ma), and compositionally similar to, the Karoo dyke swarms (Cingolani & Varela 1976; Mussett & Taylor 1994), suggesting that this continental block was still adjacent to the eastern end of the Cape Fold Belt of southern Africa in Early Jurassic times, although it was most probably attached to Patagonia by the Early Cretaceous (Mussett & Taylor 1994). Palaeomagnetic results in central Patagonia provide evidence for 25-30º clockwise rotation of tens-of-kilometre sized crustal blocks during the Late Jurassic-Early Cretaceous, similar in timing with other clockwise microplate rotations in southwestern Gondwana (Geuna *et al.* 2000 and references therein). Although the tighter fit produced with the model of Rapela & Pankhurst (1992) may alleviate some reconstruction space constraints, the amount of dextral displacement needed along a single fault system (~ 500 km) is unrealistic (Rapela 1997). Many of the problems in pre-Cretaceous reconstructions of the South

Atlantic arise because fits have been carried out using the present-day geographical boundaries of the continental fragments. However these boundaries are actually the result of large displacement of microplates that occurred during western Gondwana break-up, the formation of large sedimentary basins and the crustal extension during Cretaceous-Tertiary times (see also Jacques 2003). Relatively simple palinspastic reconstructions such as those recommended by MacDonald *et al.* (1998), produce a "tight fit" that takes into account these distorting factors, and can better explain the pre-Late Jurassic geological arrangement (Fig. 10).

Conclusions

Subduction related magmatism occurred along the southwestern (proto-Pacific) margin of Gondwana episodically over the period of more than 50 Ma prior to establishment of the Andean geotectonic cycle. The Late Triassic Batholith of Central Patagonia and the coeval metasedimentary rocks of the accretionary prism represent the last supercontinent convergence episode in the proto-Pacific margin of Patagonia. In contrast, the Early Jurassic SCB plutonic belt appears to indicate the re- establishment of subduction-related marginal magmatism farther west, simultaneously with the earliest phase of rhyolite volcanism in Patagonia and the Antarctic Peninsula, as the impingement of the Karoo mantle plume and Ferrar magmatism heralded the break-up of Gondwana. An extension interval, without obvious marginal magmatism, occurred during the Mid Jurassic stage of Chon Aike volcanism, but subduction finally resumed with the arc in the fixed position occupied by the Andean Patagonian batholith about 150 Ma, some 10-12 Ma prior to formation of the South Atlantic Ocean. Clockwise rotation through about 30° of the axis of Pacific marginal magmatism occurred during the interval 240-150 Ma, together with significant westward migration as each new episode took place. The explanation for this is not understood in detail, but has significance for the dynamics of the break up process and must involve extensive rearrangement of fragments and segments of the pre-existing continental crust.

The scenario depicted in Fig 10 does not take account of the recent reconstruction of Ghidella *et al.* (2002), in which the AP is shown as lying alongside Patagonia to the west, reaching as far north as Isla Madre de Dios, until about 160 Ma, which we find difficult to reconcile with the evidence

cited above. Their model is based on the geophysical data for opening of the Weddell sea to the southeast, and it treats both Patagonia and the Antarctic Peninsula as a rigid entities in their present-day form, which is against geological evidence indicating that important changes have occurred in both crustal blocks since Late Jurassic times (Fig. 10). In particular, the possibility that considerable parts of the Antarctic Peninsula grew by terrane accretion during the Jurassic-Cretaceous times (Vaughan & Storey 2000) could negate this conclusion. It should also be remembered that subduction-erosion may have heavily modified the form of the continental margin, removing the most external units and allowing Cretaceous portions of the batholiths to reach the coast (the trench?) south of 50°S.

Funding for this work was provided by a Leverhulme Trust Emeritus Fellowship award to RJP and by CONICET grant PIP 02082 to CWR. We are indebted to Alfredo Benialgo for preparing the digital basis of Fig. 2, and to Tim Brewer and Tom Fleming for helpful reviews.

References

Archangelsky, S. 1990. Plant distribution in Gondwana during the Late Paleozoic. In: Taylor, T.N. & Taylor, E. (eds), *Antarctic Paleobiology: its role in the reconstruction of Gondwana*. Springer-Verlag, Berlin, 102-117.

Arculus, R.J. 2003. Use and abuse of the terms calcalkaline and calcalkalic. *Journal of Petrology*, **44**, 929-935.

Artabe, A.E., Morel, E.M. & Spalletti, L.A. 2003. Caracterización de las provincias fitogeográficas triásicas del Gondwana extratropical. *Ameghiniana*, **40**, 387-405.

Bruce, R.M. 1988. Petrochemical evolution and physical construction of an Andean arc: evidence for the southern Patagonian batholith at 53º S. Ph.D. Thesis, Colorado School of Mines.

Bruce, R.M., Nelson, E.P., Weaver, S.G. & Lux, D.R. 1991. Temporal and spatial variations in the southern Patagonian batholith; Constraints on magmatic arc development. In: Harmon, R.S. & Rapela, C.W. (eds), *Plutonism from Antarctica to Alaska*, Geological Society of America Special Papers, **265**, 1-12.

Busteros, A., Franchi, M. & Lema, H.A. 1993. El magmatismo calcoalcalino del área de José de San Martín, provincia del Chubut. XII Congreso Geológico Argentino, Mendoza, Actas IV, 128-133.

Chappell, B.W. & White, A.J.R. 1992. I- and S-type granites in the Lachlan Fold Belt. *Transactions of the Royal Society of Edinburgh*, **83**, 1-26.

Cingolani, C.A. & Varela, R. 1976. Investigaciones geológicas y geocronológicas en el extremo sur de la Isla Gran Malvina, sector de Cabo Belgrano (Cabo Meredith). VI Congreso Geológico Argentino, Bahia Blanca, Actas I, Asociación Geológica Argentina, Buenos Aires, 457-480.

Cingolani, C., Dalla Salda, L., Hervé, F., Munizaga, F., Pankhurst, R.J., Parada, M.A. & Rapela, C.W. 1991. The magmatic evolution of northern Patagonia; new impressions of pre-Andean and Andean tectonics. In: Harmon, R.S. & Rapela, C.W. (eds), *Plutonism from Antarctica to Alaska*, Geological Society of America Special Papers, **265**, 29-44.

Cox, K.G. 1992. Karoo igneous activity, and the early stages of the break-up of Gondwanaland. In: Storey, B.C., Alabaster, T. & Pankhurst, R.J. (eds), *Magmatism and the causes of continental break-up*. Geological Society, London, Special Publications, **68**, 137-148.

Curtis, M.L. & Hyam, D.M. 1998. Late Palaeozoic to Mesozoic structural evolution of the Falkland Islands: a displaced segment of the Cape Fold Belt. *Journal of the Geological Society, London,* **155**, 115-129.

Dalziel, I.W.D. 1981. Back-arc extension in the southern Andes, a review and critical reappraisal. *Philosophical Transactions of the Royal Society of London,* **A300**, 319-335.

DePaolo, D. J., Linn, A. M., Schubert, G., 1991. The continental crustal age distribution; methods of determining mantle separation ages from Sm-Nd isotopic data and application to the Southwestern United States. *Journal of Geophysical Research,* **B96**, 2071-2088.

Drummond, M.S., Defant, M.J. & Kepzhinskas, P.K. 1996. Petrogenesis of slab-derived trondhjemite-tonalite-dacite/adakite magmas. *Transactions of the Royal Society of Edinburgh,* **87**, 205-215.

Duncan, R.A., Hooper, P.R., Rehacek, J., Marsh, J.S. & Duncan, A.R. 1997. The timing and duration of the Karoo igneous event, southern Gondwana. *Journal of Geophysical Research,* **B102**, 18127-18138.

Eby, G.N. 1990. The A-type granites: A review of their occurrence and chemical characteristics and speculations on their petrogenesis. *Lithos,* **26**, 115-134.

Elliot, D.H. & Fleming, T.H. 2000. Weddell triple junction: the principal focus of Ferrar and Karoo magmatism during initial breakup of Gondwana. *Geology*, **28**, 539-542.

Encarnación, J., Fleming, T.H., Elliot, D.H. & Eales, H.V. 1996. Synchronous emplacement of Ferrar and Karoo dolerites and the breakup of Gondwana. *Geology*, **24**, 535-538.

Féraud, G., Alric, V., Fornari, M., Bertrand, H. & Haller, M. 1999. $^{40}Ar/^{39}Ar$ dating of the Jurassic volcanic province of Patagonia: migrating magmatism related to Gondwana break-up and subduction. *Earth and Planetary Science Letters*, **172**, 83-96.

Forsythe, R. 1981. Geological investigations of pre-Late Jurassic terranes in the southernmost Andes. Ph.D. Thesis, Columbia University.

Forsythe, R. 1982. The late Palaeozoic and Early Mesozoic evolution of southern South America: a plate tectonic interpretation. *Journal of the Geological Society of London*, **139**, 671 - 682.

Franchi, M.R. & Page, R.F.N, 1980. Los basaltos cretácicos y la evolución magmática del Chubut occidental. *Revista de la Asociación Geológica Argentina*, **35**, 208-229.

Geuna, S.E., Somoza, R., Vizán, H., Figari, E.G. & Rinaldi, C.A. 2000. Paleomagnetism of Jurassic and Cretaceous rocks in central Patagonia: a key to constraint the timing of rotations during the breakup of Gondwana? *Earth and Planetary Science Letters*, **181**, 145-160.

Ghiara, M.R., Barbieri, M., Stanzione, D., Haller, M.J., Castorina, F., Menditti, I. & Trudu, C. 1997. Inference from basalt-rhyolite dyke swarms on the petrogenesis of a granodiorite to leucogranite suite from Patagonian Batholith (42.40º - 42.50º Lat.S). *Mineralogica Petrografica Acta*, **15**, 117-136.

Ghidella, M.E., Yañez, G. & LeBreque, J.L. 2002. Revised tectonic implications for the magnetic anomalies of the western Weddell Sea. *Tectonophysics*, **347**, 65-86.

Godeas, M. 1993. Geoquímica y marco tectónico de los granitoides en el Bajo de La Leona (Formación la Leona), provincia de Santa Cruz. *Revista de la Asociación Geológica Argentina*, **47**, 347-347.

González Bonorino, G. 1990. Cambios relativos en el nivel del mar y su posible relación con magmatismo en el Jurásico temprano, Formación Lepa, Chubut noroccidental, Argentina. *Revista de la Asociación Geológica Argentina*, **45**, 129-135.

González Díaz, E.F. 1982. Chronological zonation of granitic plutonism in the northern Patagonian Andes of Argentina: the migration of intrusive cycles. *Earth Science Reviews*, **18**, 365-393.

Gordon, A. & Ort, M.H. 1993. Edad y correlación del plutonismo subcordillerano en las provincias de Río Negro y Chubut (41º -42º 30'L.S.). XII Congreso Geológico Argentino, Mendoza, Actas IV, 120-127.

Gorring, M. L. & Kay, S.M. 2001. Mantle processes and sources of Neogene slab window magmas from southern Patagonia, Argentina. *Journal of Petrology*, **42**, 1067-1094.

Haller, M.J. 1985. El magmatismo Mesozoico en Trevelin, Cordillera Patagónica, Argentina. 4° Congreso Geológico Chileno, Antofagasta, Actas 3, 215-234.

Haller, M.J., Linares, M., Ostera, H.A. & Page, S.M. 1999. Petrology and geochronology of the Subcordilleran Plutonic Belt of Patagonia, Argentina. II South American Symposium on Isotope Geology, Carlos Paz, Argentina, Actas, 210-214.

Hervé, F. & Fanning, C.M. 2003. Early Cretaceous subduction of continental crust at the Diego de Almagro archipelago, southern Chile. *Episodes*, **26**, 285-289.

Hervé, F., Pankhurst, R.J., Suárez, M. & de la Cruz, R. 1993. Basic magmatism in a mid-Tertiary transtensional basin, Isla Magdalena, Aysén, Chile. Second Symposium International, Géodynamique Andine, Oxford (21-23 September 1993), Éditions de l'ORSTOM, Colloques et Séminaires, Paris 1993, 367-369.

Hervé, F., Fanning, C.M. & Pankhurst, R.J. 2003. Detrital Zircon Age Patterns and Provenance of the metamorphic complexes of Southern Chile. *Journal of South American Earth Sciences*, **16**, 107-123.

Irvine, T.N. & Baragar, W.R. 1971. A guide to the chemical classification of the common igneous rocks. *Canadian Journal of Earth Sciences*, **8**, 523-548.

Jacques, J.M. 2003. A tectonostratigraphic synthesis of the sub-Andean basins; inferences on the position of South American intraplate accommodation zones and their control on South Atlantic opening. *Journal of the Geological Society, London*, **160**, 703-717.

Kay, S.M., Ramos, V.A. & Marquez, M. 1993. Evidence in Cerro Pampa volcanic rocks for slab-melting prior to ridge-trench collision in southern South America. *Journal of Geology*, **101**, 703-714.

Kraemer, P. 2003. Orogenic shortening and the origin of the Patagonian Orocline (56°S Lat.). *Journal of South American Earth Sciences*, **15**, 731-748.

Ling, H.Y., Forsythe, R.D., Douglas, C.R.. 1987. Late Paleozoic microfaunas from southernmost Chile and their relation to Gondwanaland forearc development. *Geology*, **13**, 357-360.

Lizuaín, A. 1981. Características y edad del plutonismo en los alrededores del lago Puelo-Provincia del Chubut. VIII Congreso Geológico Argentino, San Luis, Actas 3, 607-616.

Lizuaín, A. 1983. Geología de la Cordillera Patagónica entre las localidades de Lago Puelo y Leleque. Ph.D. thesis, Universidad de Buenos Aires, unpublished.

Lizuaín, A. 1999. El Jurásico y Cretácico de la Patagonia y Antártida. 1. Estratigrafía y evolución geológica del Jurásico y Cretácico de la Cordillera Patagónica Septentrional. *In*: Caminos, R. (ed.), *Geología Argentina*, Subsecretaría de Minería de la Nación, Servicio Geológico Minero Argentino, Instituto de Geología y Recursos Minerales, Anales Nº 29, 433-443.

Ludwig. K.R. 1999. Isoplot/Ex, a geochronological toolkit for Microsoft Excel. Berkeley Geochronological Center Special Publication No. 1. version 2.31. 2455 Ridge Road, Berkeley, CA 94709.

Ludwig, K.R. 2001. Squid 1.00. A User's Manual, Berkeley Geochronology Center Special Publication No. 2. 2455 Ridge Road, Berkeley CA 94709.

MacDonald, D., Gomez-Perez, I., Franzese, J., Spalletti, L., Paton, D., Gilpin, R. & Andersen, L. 1998. Mesozoic evolution of the South Atlantic and its influence on the Tertiary development of the region. South Atlantic Project, Report No. 10, Cambridge Artic Shelf Programme (CASP)-Centro de Investigaciones Geológicas (CIG).

Marshall, J.E.A. 1994. The Falkland Islands: a key element in Gondwana paleogeography. *Tectonics*, **13**, 499-514.

Martin, M., Pankhurst, R.J., Fanning, C.M., Thomson, S.N., Calderón, M. & Hervé, F. 2001. Age distribution of plutons across the southern Patagonian batholith: new U-Pb age data on zircons. Third South American Symposium of Isotope Geology, Pucón, Chile. CD-ROM, SERNAGEOMIN, Santiago, 585-588.

Mitchell, C., Taylor, G.K., Cox, K.G. & Shaw, J. 1986. Are the Falkland Islands a rotated microplate? *Nature*, **319**, 131-134.

Mukasa, S.B. & Dalziel, I.W.D. 1996. Southernmost Andes and South Georgia Island, north Scotia Ridge: zircon U-Pb and muscovite $^{40}Ar/^{39}Ar$ age constraints on tectonic evolution of southwestern Gondwanaland. *Journal of South American Earth Sciences*, **9**, 349-365.

Mussett, A.E. & Taylor, G.K. 1994. ^{40}Ar-^{39}Ar ages of dykes from the Falkland Islands with implications for the break-up of southern Gondwanaland. *Journal of the Geological Society, London,* **151**, 79-81.

Olivares, B., Cembrano, J., Hervé, F., López, G., Prior, D. 2003. Análisis estructural de rocas de una zona de cizalle dúctil en isla Diego de Almagro, sur de Chile. *Revista Geológica de Chile*, **309**, 39-52.

Page, S. & Page, R. 1999. Las diabasas y gabros del Jurásico de la Precordillera del Chubut. *In*: Caminos, R. (ed.), *Geología Argentina*, Subsecretaría de Minería de la Nación, Servicio Geológico Minero Argentino, Instituto de Geología y Recursos Minerales, Anales No. 29, 489-495.

Palmer, A.R. & Geissman, J. (compilers) 1999. *The 1999 Geologic Time Scale*. Geological Society of America, Boulder, CO.

Pankhurst, R.J. 1982. Rb-Sr geochronology of Graham Land, Antarctica. *Journal of the Geological Society*, **139**, 701-711.

Pankhurst, R.J. & Rapela, C.W. 1995. Production of Jurassic rhyolite by anatexis in the lower crust of Patagonia. *Earth and Planetary Science Letters*, **134**, 23-36.

Pankhurst, R..J., Rapela, C.W., Caminos, R., Llambías, E.J. & Párica, C. 1992. A revised age for the granites of the central Somuncura batholith, North Patagonian Massif. *Journal of South American Earth Sciences*, **5**, 321-325.

Pankhurst, R.J., Rapela, C.W. & Márquez, M. 1993. Geocronología y petrogénesis de los granitoides jurásicos del noreste del Macizo del Deseado. XII Congreso Geológico Argentino, Mendoza, Actas IV, 134-141.

Pankhurst, R.J., Hervé, F. & Rapela, C.W. 1994. Sm-Nd evidence for the Grenvillian provenance of the metasedimentary basement of Southern Chile and West Antarctica. *In*: E. Campos & A. Cecioni (eds), Actas del VII Congreso Geológico Chileno, Vol. II, Universidad del Norte Chile, Departamento de Geociencias, Facultad de Ciencias. Antofagasta, Chile, 1414-1418.

Pankhurst, R.J., Leat, P.T., Sruoga, P, Rapela, C.W., Márquez, M., Storey, B.C. & Riley, T.R. 1998. The Chon-Aike silicic igneous province of Patagonia and related rocks in West Antarctica: a silicic LIP. *Journal of Volcanology and Geothermal Research*, **81**, 113-136.

Pankhurst, R.J., Weaver, S.D., Hervé, F. & Larrondo, P. 1999. Mesozoic-Cenozoic evolution of the North Patagonian Batholith in Aysén, southern Chile. *Journal of the Geological Society, London*, **156**, 673-694.

Pankhurst, R.J., Riley, T.R., Kelley, S. & Fanning, C.M. 2000. Episodic silicic volcanism in Patagonia and the Antarctic Peninsula: chronology of magmatism associated with the break-up of Gondwana. *Journal of Petrology*, **41**, 605-625.

Pankhurst, R.J., Hervé, F., Fanning, C.M. & Suárez, M. 2003a. Coeval plutonic and volcanic activity in the Patagonian Andes: the Patagonian Batholith and the Ibáñez and Divisadero Formations, Aysén, southern Chile. X Congreso Geológico Chileno, Actas (CD-ROM).

Pankhurst, R.J., Rapela, C.W., Loske, W.P., Fanning, C.M. & Márquez, M. 2003b. Chronological study of the pre-Permian basement rocks of southern Patagonia. *Journal of South American Earth Sciences*, **16**, 27-44.

Pearce, J.A. 1983. Role of the sub-continental lithosphere in magma genesis at active continental margins. In: Hawkesworth, C.J. & Norry, M.J. (eds.), *Continental basalts and mantle xenoliths*. Shiva, Nantwich, U.K., 230-249.

Pearce, J.A., Harris, N.B.W. & Tindle, A.G. 1984. Trace element discrimination diagrams for the tectonic interpretation of granitic rocks. *Journal of Petrology*, **25**, 956-983.

Rapalini, A.E., Hervé, F., Ramos, V.A. & Singer, S. 2001. Paleomagnetic evidence of a very large counterclockwise rotation of the Madre de Dios archipelago, southern Chile. *Earth and Planetary Science Letters*, **184**, 471-487.

Rapela, C.W. 1997. El sistemas de fallas de Gastre: e pur si muove. *Revista de la Asociación Geológica Argentina*, **52**, 219-222.

Rapela, C.W. 2001. El magmatismo Triásico-Jurásico de la Patagonia y su ambiente geodinámico. In: Artabe, A.E., Morel E.M. & Zamuner, A.B. (eds.), *El Sistema Triásico en la Argentina*. Fundación Museo de La Plata 'Francisco Pascasio Moreno', La Plata, 69-80.

Rapela, C.W. & Kay, S. 1988. The Late Paleozoic to Recent magmatic evolution of northern Patagonia. *Episodes*, **11**, 175-182.

Rapela, C.W. & Pankhurst, R.J. 1992. The granites of northern Patagonia and the Gastre Fault System in relation to the break-up of Gondwana. *In*: Storey, B.C., Alabaster, T. & Pankhurst, R.J. (eds), *Magmatism and the Causes of Continental Break-up*. Geological Society Special Publications, **68**, 209-220.

Rapela, C.W. & Pankhurst, R.J. 1996. Monzonite Suites: the innermost Cordilleran plutonism of Patagonia. *Transactions of the Royal Society of Edinburgh, Earth Sciences*, **87**, 193-203.

Rapela, C.W., Pankhurst, R.J. & Harrison, S.M. 1992. Triassic "Gondwana" granites of the Gastre district, North Patagonian Massif. *Transactions of the Royal Society of Edinburgh, Earth Sciences*, **83**, 291-304.

Rapela, C.W., Pankhurst, R.J., Llambías, E.J., Labudía, C. & Artabe, A. 1996. "Gondwana" magmatism of Patagonia: Inner Cordilleran calc-alkaline batholiths and bimodal volcanic provinces. 3rd. International Symposium on "Andean Geodynamics", Saint Malo, Extended Abstracts, 791-794.

Rapela, C.W., Pankhurst, R.J., Fanning, C.M. & Grecco, L.E., 2003. Basement evolution of the

Sierra de la Ventana Fold Belt: new evidence for Cambrian continental rifting along the southern margin of Gondwana. *Journal of the Geological Society*, **160**, 613-628.

Remane, J., Faure-Muret, A. & Odin, G.S. (compilers) 2000. International Stratigraphic Chart, International Union of Geological Sciences.

Riley, T.R., Leat, P.T., Pankhurst, R.J. & Harris, C. 2001. Origins of large-volume rhyolite volcanism in the Antarctic Peninsula and Patagonia by crustal melting. *Journal of Petrology*, **42**, 1043-1065.

Riley, T.R., Millar, I.L., Watkeys, M.K., Curtis, M.L., Leat, P.T., Klausen, M.B. & Fanning, C.M. 2004. U–Pb zircon (SHRIMP) ages for the Lebombo rhyloites, South Africa: refining the duration of Karoo volcanism. *Journal of the Geological Society*, **161**, 547-550.

Rolando, A.P., Hartmann, L.A., Santos, J.O.S., Fernandez, R.R., Etcheverry, R.O., Schalamuk, I.A. & McNaughton, N.J. 2002. SHRIMP zircon U-Pb evidence for extended Mesozoic magmatism in the Patagonian batholith and assimilation of Archaean crustal components. *Journal of South American Earth Sciences*, **15**, 267-283.

Söllner, F., Miller, H. & Hervé, M. 2000. An Early Cambrian granodiorite age from the pre-Andean basement of Tierra del Fuego (Chile): the missing link between South America and Antarctica? *Journal of South American Earth Sciences*, **13**, 163-177.

Spikermann, J.P. 1978. Contribución al conocimiento de la intrusividad en el paleozoico de la región extrandina de Chubut. *Revista Asociación Geológica Argentina*, **23**, 17-35.

Spikermann, J.P., Strelin, J., Marshall, P., Carrillo, R., Montenegro, T., Lago, M., Villalba, E. & Pérez, A. 1988. Geología del área El Batolito Aleusco, Departamento de Languiñeo, provincia de Chubut. *Revista de la Asociación Argentina de Mineralogía, Petrología y Sedimentología*, **19**, 39-48.

Spikermann, J.P., Strelin, J., Marshall, P., Carrillo, R., Montenegro, T., Lago, M., Villalba, E. & Pérez, A. 1989. Caracterización geológica del Batolito Aleusco, Departamento de Languiñeo,

provincia, provincia de Chubut. *Revista de la Asociación Argentina de Mineralogía, Petrología y Sedimentología*, **20**, 33-42.

Stern, Ch.R. & Kilian, R. 1996. Role of the subducted slab, mantle wedge and continental crust in the generation of adakites from the Andean Austral Volcanic Zone. *Contributions to Mineralogy and Petrology*, **123**, 263-281.

Storey, B.C. 1995. The role of mantle plumes in continental break-up: case histories from Gondwanaland. *Nature*, **377**, 301-308.

Storey, B.C., Alabaster, T., Hole, M.J., Pankhurst, R.J. & Wever, H.E. 1992. Role of subduction-plate boundary forces during the initial stages of Gondwana breakup: evidence from the proto-Pacific margin of Gondwana. *In*: Storey, B.C., Alabaster, T. & Pankhurst, R.J. (eds) *Magmatism and the Causes of Continental Break-up*. Geological Society, London, Special Publications, **68**, 149-163.

Suárez, M. & De La Cruz, R. 1997a. Edades K–Ar del grupo Ibáñez en la parte oriental del Lago General Carrera (46°–47° LS), Aysén, Chile. VIII Congreso Geológico Chileno, Antofagasta, Chile. Vol. 2. 1548-1551.

Suárez, M. & De La Cruz, R. 1997b. Cronologia magmática de Aysén sur (45°–48°30' L.S.), Aysén, Chile. VIII Congreso Geológico Chileno, Antofagasta, Chile. Vol. 2. 1543-1547.

Suarez, M. & De la Cruz, R. 2001. Jurassic to Miocene K-Ar dates from eastern central Patagonian Cordillera plutons, Chile (45º-48º S). *Geological Magazine*, **138**, 53-66.

Taylor, G.K. & Shaw, J. 1989. *The Falkland Islands: new palaeomagnetic data and their origin as a displaced terrane from southern Africa*. American Geophysical Union, Geophysical Monograph, **50**, 59-72.

Thompson, R.N., Morrison, M.A., Hendry, G.L. & Parry, S.J. 1984. An assessment of the relative roles of the crust and mantle in magma genesis: an elemental approach. *Philosophical Transactions of the Royal Society, London*, Series **A310**, 549-590.

Thomson, S.N. & Hervé, F. 2002. New time constraints for the age of metamorphism at the ancestral Pacific Gondwana margin of southern Chile (42-52ºS). *Revista Geológica de Chile*, **29**, 255-271.

Turner, J.C. 1982. Descripción geológica de la Hoja 44c, Tecka, provincia del Chubut. Servicio Geológico Nacional, Boletín 180.

Turner, S., Regelous, M., Kelley, S., Hawkesworth, C. & Mantovani, M. 1994. Magmatism and continental break-up in the South Atlantic: high precision ^{40}Ar-^{39}Ar geochronology. *Earth and Planetary Science Letters*, **121**, 333-348.

Uliana, M.A. & Legarreta, L. 1999. Jurásico y Cretácico de la cuenca del Golfo de San Jorge. *In*: Caminos, R. (ed.), *Geología Argentina*, Subsecretaría de Minería de la Nación, Servicio Geológico Minero Argentino, Instituto de Geología y Recursos Minerales, Anales Nº 29, 496-510.

Vaughan, A.P.M. & Storey, B.C. 2000. The eastern Palmer Land shear zone: a new terrane accretion model for the Mesozoic development of the Antarctic Peninsula. *Journal of the Geological Society, London*, **157**, 1243-1256.

Weaver, S.G. 1988. The Patagonian batholith at 48ºS latitude, Chile: implication for the petrochemical and geochemical evolution of calc-alkaline batholiths. Ph.D. Thesis, Colorado School of Mines.

Wells, P. 1978. The geochemistry of the Patagonian batholith between 45ºS and 46ºS latitude. MSc. Thesis, University of Birmingham.

Whalen, J.B., Currie, K.L. & Chappell, B.W. 1987. A-type granites: geochemical characteristics, discrimination and petrogenesis. *Contributions to Mineralogy and Petrology*, **95**, 407-419.

Williams, I.S. 1998. U-Th-Pb Geochronology by Ion Microprobe. In: McKibben, M.A., Shanks, W.C. III & Ridley, W.I. (eds), Applications of microanalytical techniques to understanding mineralizing processes. *Reviews in Economic Geology*, **7**, 1-35.

Zindler, A. & Hart, S.R. 1986. Chemical geodynamics. *Annual Review of Earth and Planetary Sciences*, **14**, 493-571.

Figure Captions

Figure 1: Distribution of Triassic and Jurassic magmatism and location of the main sedimentary basins in Patagonia (modified from Rapela 2001). The boundary of the Subcordilleran belt (cross-hached area inside the box) is after the palaeogeographic reconstruction of the Liassic basin by Lizuaín (1999), while the main areas of the Triassic–Early Jurassic accretionary prism in the Pacific margin are from Thomson & Hervé (2002). Isotopic ages for the Chon Aike province are from Pankhurst *et al.* (2000): rocks of V1 (188-178 ~) occur in the eastern North Patagonian Massif; those of V_2 (~172–162 Ma) and V_3 (~157–153 Ma and younger) are not distinguished. See text for data sources and discussion of the isotopic ages of the I-type granites: the coastal batholith (and the sedimentary basins outlined) are largely post-break up.

Figure 2: Simplified geological map of the Subcordilleran sector between 41º 30´and 44º 15´S.

Figure 3: Normative Ab-An-Or diagram for the Mesozoic and Cenozoic I-type granites of Patagonia. Data for the Subcordilleran belt are from Gordon & Ort (1993), Busteros *et al.* (1993), Haller *et al.* (1999) and this paper; for the Deseado Monzonite Suite from Rapela *et al.* (1996); and for the Batholith of Central Patagonia from Rapela *et al.* (1992). The normative composition of the Patagonian batholith is based on 415 chemical analyses reported for different latitudes of the body: 53ºS (Bruce, 1988), 48ºS (Weaver 1988), 45º - 46ºS (Wells, 1978), 44º - 46ºS (Pankhurst *et al.* 1999), 43ºS (Haller 1985), 42º (Ghiara *et al.* 1997) and 40–41ºS (Rapela 1987, and unpublished data).

Figure 4: Reflected light and cathodo-luminescence images of analysed zircon grains from sample SER-046 (La Angostura granite). The large grain is *c.* 250 μm in length. SHRIMP ablation spots are marked on the left-hand image, chosen to avoid cracks and inclusions.

Figure 5: Tera-Wasserburg plots of SHRIMP zircon data for magmatic units of the Subcordilleran plutonism of northwestern Patagonia. Open ellipses are 68% confidence limits for analyses of crystal tips, uncorrected for common Pb. Age errors are reported at 95% confidence limit. Shaded ellipses are for data outside the acceptable range for definition of a single event,

probably due to either minor inheritance of older Pb or radiogenic Pb-loss; these were excluded from the calculation of crystallization ages.

Figure 6: Harker plots for Triassic-Jurassic I-type granites and volcanic rocks from Patagonia. The line dividing alkaline and subalkaline fields is from Irvine & Baragar (1971) while the fields for high-, medium- and low-Fe are after Arculus (2003). Data sources for the Triassic and Jurassic volcanic rocks: Pankhurst & Rapela (1995); Rapela (2001) and unpublished data from a British Antarctic Survey – Argentine joint expedition (P.T. Leat, pers. comm. 2003). Data sources for the I-type granites are the same as reported in Fig. 3.

Figure 7: (a) Trace element abundances in granitic rocks of the Subcordilleran belt normalized to ocean ridge granite (ORG, Pearce *et al.* 1984). The field of the Patagonian batholith has been constructed from chemical data for hornblende-biotite granodiorites and tonalites (61–69 % SiO_2) reported by Ghiara *et al.* (1997), Pankhurst *et al.* (1999), and unpublished data of C.W. Rapela at 41º S; (b) Trace element abundances in granitic and basic rocks of the Subcordilleran belt normalized to MORB (Pearce 1983); (c) Chondrite-normalized REE patterns of representative samples from the Subcordilleran plutonic belt.

Figure 8: Variation of εNdt versus initial $^{87}Sr/^{86}Sr$ for the Late Triassic and Jurassic magmatic units of Patagonia. Data sources for I-type granites: Rapela *et al.* 1992; Rapela & Pankhurst 1996; Pankhurst *et al,* 1999 and Pankhurst, R.J. & Hervé, F., unpublished data; for volcanic rocks: Pankhurst & Rapela 1995 and Pankhurst, R.J., unpublished data. The fields for the upper and lower crust in Fig. 7c are from the Chilean accretionary prism and the North Patagonian Massif V_1 rhyolite group respectively (Pankhurst *et al.* 1999). MORB (mid-ocean ridge basalts) field is from Zindler & Hart (1986), while SVZ (mafic Southern Volcanic Zone) is from Gorring & Kay (2001 and references therein).

Figure 9: Histograms of ages for the Mesozoic and Cenozoic I-type granites of Patagonia. Data sources: Patagonian batholith between 45– 53º S (Bruce *et al.* 1991; Pankhurst *et al.* 1999; Suarez & De la Cruz 2001); Subcordilleran belt (Lizuaín 1981; Gordon & Ort 1993; Haller *et al.* 1999; this paper); Deseado Monzonite Suites (Pankhurst *et al.* 1993); Batholith of Central

Patagonia (Rapela *et al.* 1992). Cumulative probability curve and age groups for the Jurassic rhyolite province of Patagonia is from Pankhurst *et al.* (2000). Inferred ages for the Karoo and Tristan mantle plumes are from Duncan *et al.* (1997) and Turner *et al.* (1994) respectively.

Figure 10: Schematic Early Jurassic palaeogeographical reconstruction of southwestern Gondwana (modified after the Early Jurassic base map of Storey *et al.* 1992). A tight fit is obtained by a palinspastic restoration of southern South America and the Antarctic Peninsula as proposed by McDonald *et al.* (1998), involving 50% closing of the largest southernmost Mesozoic basins (Austral, San Jorge and Colorado, Fig. 1), reducing by 20 % the size of Antarctic Peninsula to remove approximately Late Mesozoic and Tertiary crustal growth, and allowing for moderate dextral displacement of about 140 km of large crustal blocks along major fault systems bounding the North Patagonian and the Deseado massifs. Partial restoration of the Cretaceous-Cenozoic oroclinal curvature in the southern tip of South America and the Antarctic Peninsula has been also performed (e.g., Kraemer 2003). Triassic and Early Jurassic accretionary prism after Thomson & Hervé (2002). Location and timing of the Jurassic magmatic provinces is after Pankhurst *et al.* (2000), while heavy broken lines that show the sites of the initial areas of the Indian Ocean (1) and the future South Atlantic Ocean (2) are from Cox (1992). Crustal blocks: EWM, Ellsworth-Whitmore mountains; SG, South Georgia; F/M, Falkland/Malvinas microplate; TI, Thurston Island; MBL, Marie Byrd Land; New Zealand, New Zealand.

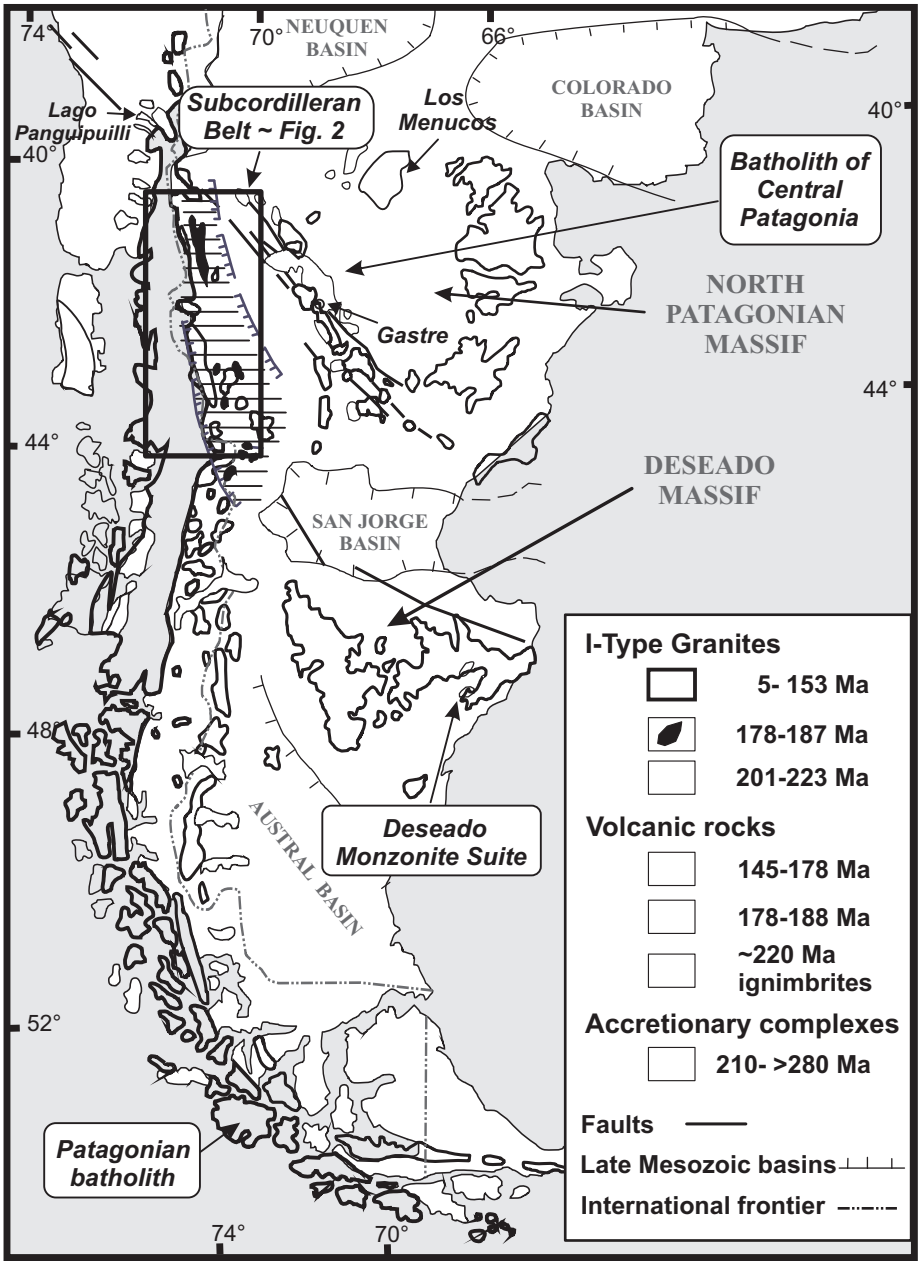

Rapela et al. Figure 1

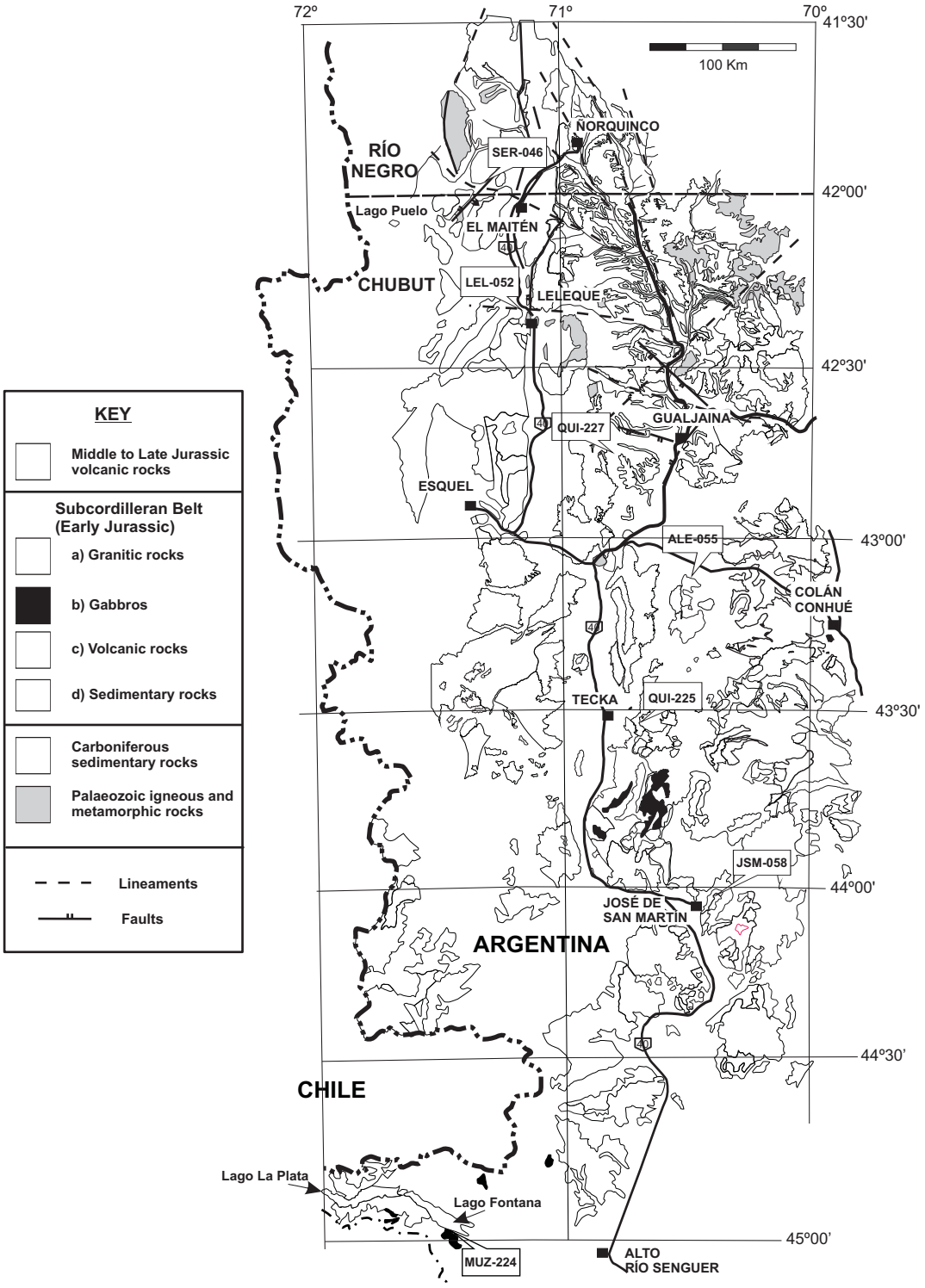

Rapela et al. Figure 2

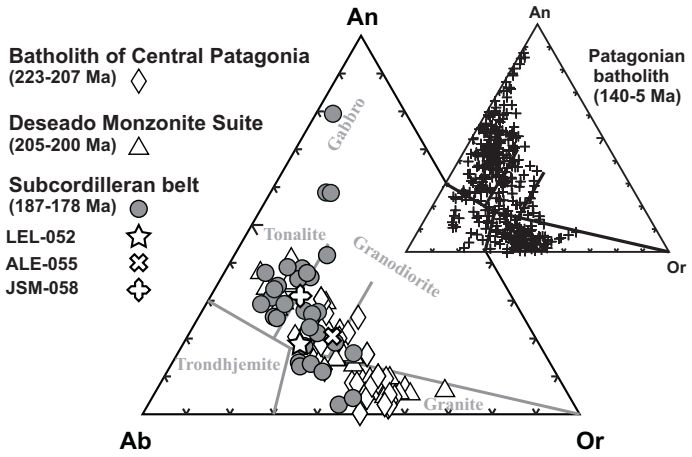

Rapela et al. Figure 3

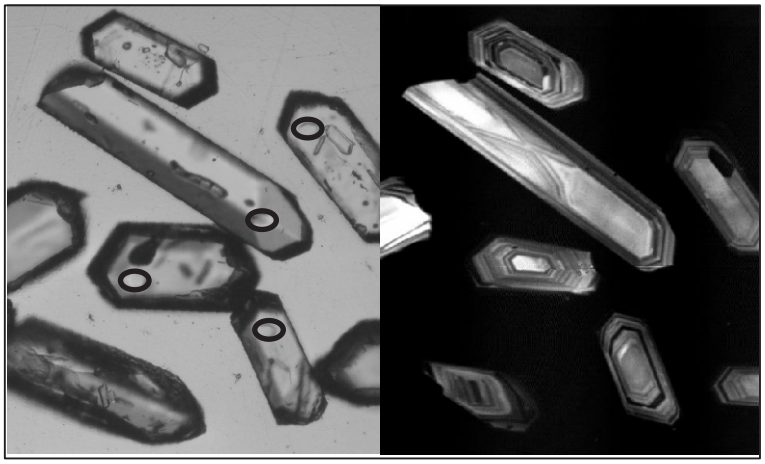

Rapela et al. Figure 4

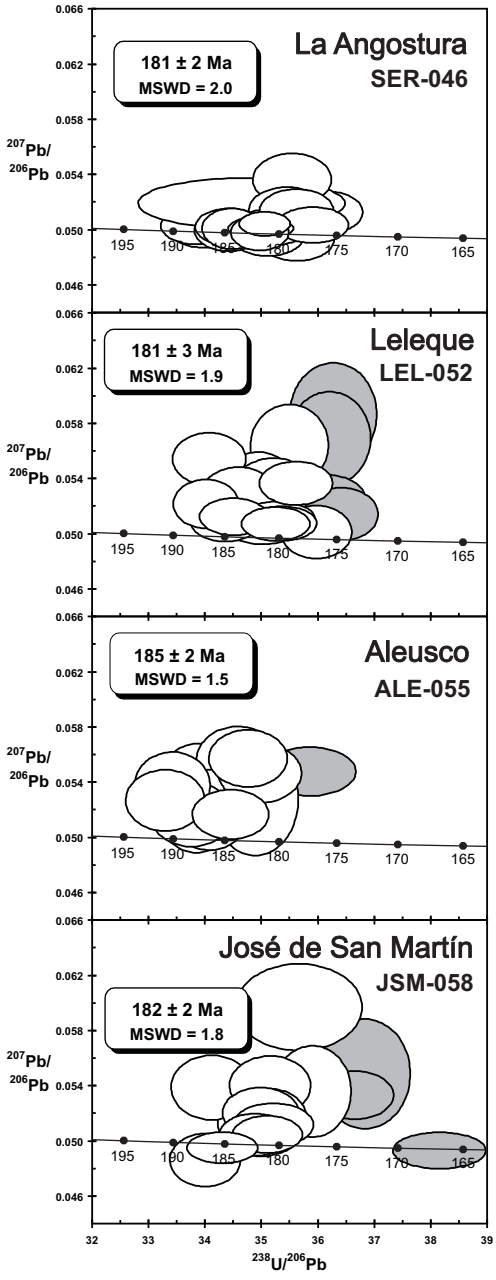

Rapela et al. Figure 5

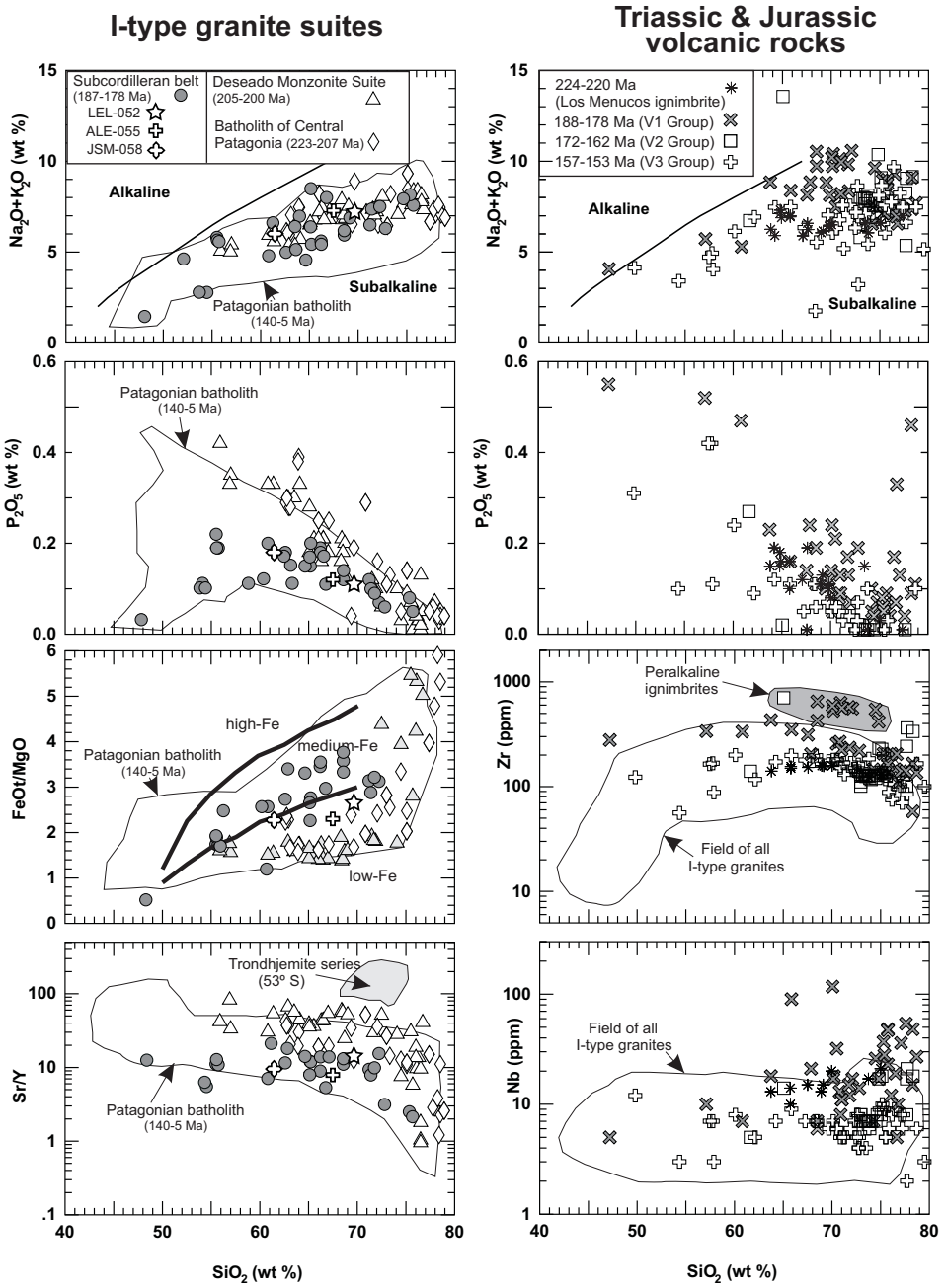

Rapela et al. Figure 6

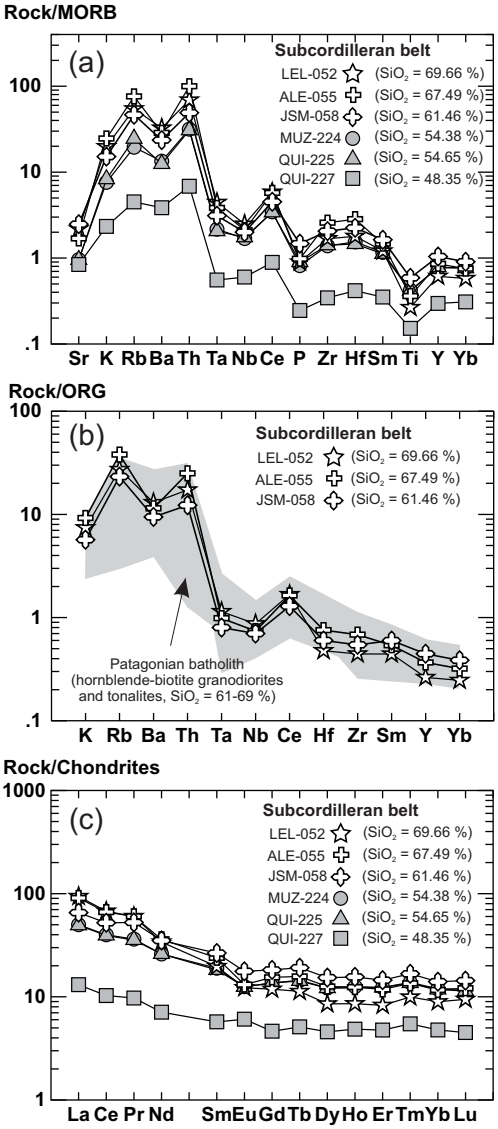

Rapela et al. Figure 7

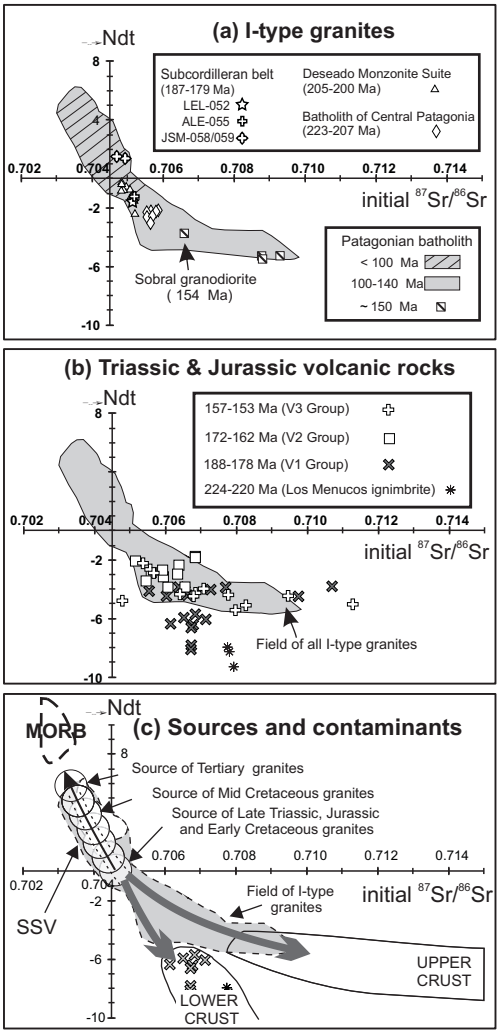

Rapela et al. Figure 8

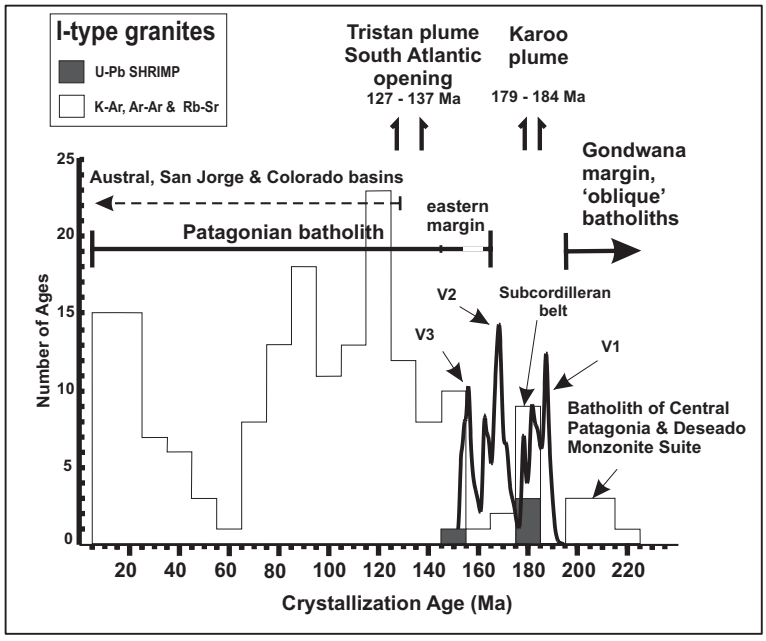

Rapela et al. Figure 9

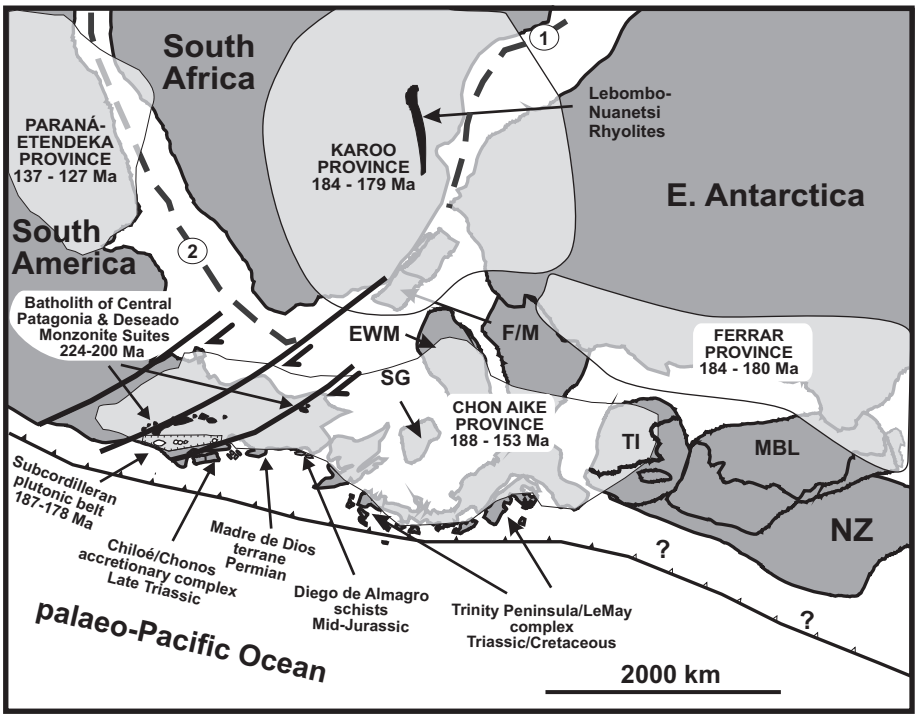

Rapela et al. Figure 10

Table 1. SHRIMP U–Pb Zircon Data

Grain. spot	U (ppm)	Th (ppm)	Th/U	$^{206}Pb^*$ (ppm)	$^{204}Pb/^{206}Pb$	f_{206} %	Total $^{238}U/^{206}Pb$	±	Total $^{207}Pb/^{206}Pb$	±	Radiogenic $^{206}Pb/^{238}U$	±	Age (Ma) $^{206}Pb/^{238}U$	±
SER-046														
1.1	598	229	0.38	14.9	0.000318	0.05	34.431	0.400	0.0501	0.0009	0.0290	0.0003	184.5	2.1
2.1	301	106	0.35	7.3	0.000313	0.49	35.531	0.459	0.0535	0.0012	0.0280	0.0004	178.1	2.3
3.1	731	313	0.43	17.9	0.000074	0.05	35.157	0.446	0.0501	0.0009	0.0284	0.0004	180.7	2.3
4.1	579	185	0.32	13.9	0.000144	0.08	35.904	0.417	0.0503	0.0008	0.0278	0.0003	176.9	2.0
5.1	466	185	0.40	11.8	0.000197	0.03	33.957	0.407	0.0501	0.0010	0.0294	0.0004	187.0	2.2
6.1	1234	634	0.51	30.3	0.000089	0.04	34.983	0.379	0.0500	0.0006	0.0286	0.0003	181.6	2.0
7.1	469	160	0.34	11.3	-	<0.01	35.623	0.436	0.0492	0.0010	0.0281	0.0003	178.6	2.2
8.1	499	206	0.41	11.9	-	0.20	36.131	0.436	0.0512	0.0010	0.0276	0.0003	175.6	2.1
9.1	360	116	0.32	8.7	0.000091	0.21	35.442	0.445	0.0513	0.0011	0.0282	0.0004	179.0	2.2
10.1	438	148	0.34	10.7	-	<0.01	35.102	0.427	0.0496	0.0010	0.0285	0.0004	181.1	2.2
11.1	462	189	0.41	11.1	0.000226	0.21	35.620	0.429	0.0513	0.0010	0.0280	0.0003	178.1	2.1
12.1	321	94	0.29	8.0	0.000181	0.26	34.643	1.208	0.0518	0.0012	0.0288	0.0010	183.0	6.3
13.1	596	229	0.39	15.1	0.000174	0.05	33.811	0.395	0.0502	0.0009	0.0296	0.0003	187.8	2.2
14.1	582	231	0.40	14.5	0.000138	0.01	34.417	0.401	0.0498	0.0010	0.0291	0.0003	184.6	2.1
15.1	409	144	0.35	10.2	0.000000	0.03	34.461	0.346	0.0500	0.0010	0.0290	0.0003	184.4	1.8
16.1	455	183	0.40	11.2	0.000109	<0.01	34.965	0.336	0.0497	0.0008	0.0286	0.0003	181.8	1.7
17.1	1150	562	0.49	28.2	0.000058	0.08	35.044	0.300	0.0504	0.0006	0.0285	0.0002	181.2	1.5
											Weighted mean age and 95% c.l. error		**181.1**	**1.7**
LEL-052														
*1.1	148	38	0.26	6.7	-	0.52	19.093	0.230	0.0572	0.0019	0.0521	0.0006	327.4	4.0
2.1	339	494	1.46	8.1	-	0.07	35.974	0.417	0.0502	0.0013	0.0278	0.0003	176.6	2.0
3.1	420	356	0.85	10.2	0.000127	0.14	35.253	0.399	0.0508	0.0008	0.0283	0.0003	180.1	2.0
4.1	361	652	1.80	9.0	0.000159	0.19	34.506	0.398	0.0513	0.0009	0.0289	0.0003	183.8	2.1
5.1	252	300	1.19	6.3	0.000039	0.15	34.361	0.412	0.0510	0.0010	0.0291	0.0004	184.7	2.2
6.1	211	244	1.16	5.2	-	0.41	34.604	0.430	0.0530	0.0012	0.0288	0.0004	182.9	2.3
7.1	195	181	0.93	4.9	-	0.71	34.080	0.431	0.0555	0.0013	0.0291	0.0004	185.1	2.3
8.1	376	268	0.71	9.2	0.000056	0.17	35.270	0.452	0.0510	0.0009	0.0283	0.0004	179.9	2.3
9.1	288	326	1.13	7.1	0.000216	0.17	35.028	0.545	0.0510	0.0011	0.0285	0.0004	181.2	2.8
10.1	458	412	0.90	11.6	0.000179	0.30	34.018	0.381	0.0522	0.0012	0.0293	0.0003	186.2	2.1
*11.1	430	358	0.83	10.1	0.000128	0.24	36.409	0.433	0.0515	0.0013	0.0274	0.0003	174.3	2.1
12.1	516	646	1.25	12.5	-	0.14	35.360	0.411	0.0508	0.0008	0.0282	0.0003	179.5	2.1
13.1	274	186	0.68	6.6	0.000131	0.51	35.620	0.428	0.0537	0.0010	0.0279	0.0003	177.6	2.1
14.1	167	170	1.02	4.1	0.000199	0.47	35.219	0.470	0.0534	0.0014	0.0283	0.0004	179.7	2.4
15.1	380	312	0.82	9.2	0.000431	0.86	35.495	0.456	0.0565	0.0019	0.0279	0.0004	177.6	2.3
*16.1	335	402	1.20	7.9	0.000749	0.92	36.203	0.482	0.0569	0.0022	0.0274	0.0004	174.0	2.4
*17.1	287	364	1.27	6.8	0.000397	1.15	36.272	0.512	0.0587	0.0025	0.0273	0.0004	173.3	2.5
18.1	462	388	0.84	11.3	0.000320	0.44	34.934	0.455	0.0532	0.0018	0.0285	0.0004	181.2	2.4
*19.1	492	485	0.99	11.7	0.000339	0.38	36.135	0.467	0.0526	0.0011	0.0276	0.0004	175.3	2.3
											Weighted mean age and 95% c.l. error (excluding points marked *)		**181.1**	**2.5**
ALE-055														
*1.1	185	90	0.49	4.4	-	0.65	35.849	0.538	0.0548	0.0012	0.0277	0.0004	176.2	2.6
2.1	182	165	0.91	4.6	0.000127	0.48	34.360	0.496	0.0536	0.0017	0.0290	0.0004	184.1	2.7
3.1	124	79	0.63	3.2	0.000331	0.35	33.295	0.460	0.0527	0.0015	0.0299	0.0004	190.1	2.6
4.1	100	57	0.57	2.5	0.000228	0.74	34.595	0.490	0.0556	0.0016	0.0287	0.0004	182.4	2.6
5.1	103	64	0.62	2.6	0.000022	0.23	33.753	0.477	0.0517	0.0015	0.0296	0.0004	187.8	2.7
6.1	146	130	0.89	3.7	-	0.49	33.414	0.443	0.0538	0.0016	0.0298	0.0004	189.2	2.5
7.1	195	148	0.76	4.9	0.000233	0.32	34.118	0.419	0.0524	0.0017	0.0292	0.0004	185.6	2.3
8.1	98	55	0.56	2.5	0.000308	0.28	34.070	0.482	0.0520	0.0019	0.0293	0.0004	186.0	2.6
*9.1	93	59	0.64	2.7	0.000687	17.65	29.331	0.460	0.1905	0.0658	0.0281	0.0030	178.5	18.5
10.1	134	111	0.83	3.3	0.000068	0.75	34.755	0.457	0.0557	0.0014	0.0286	0.0004	181.5	2.4
11.1	130	117	0.90	3.2	0.000253	0.39	34.887	0.504	0.0528	0.0027	0.0286	0.0004	181.5	2.7
12.1	142	116	0.82	3.6	-	0.38	33.851	0.497	0.0528	0.0026	0.0294	0.0004	187.0	2.8
13.1	238	243	1.02	5.9	-	0.24	34.451	0.447	0.0517	0.0012	0.0290	0.0004	184.0	2.4

14.1	148	81	0.55	3.6	-		0.62	34.975	0.487	0.0547	0.0014	0.0284	0.0004	180.6	2.5
						Weighted mean age and 95% c.l. error (excluding points marked *)								**184.9**	**2.3**

JSM-058

*1.1	95	66	0.70	2.2	0.000434	0.67	36.833	0.532	0.0548	0.0026	0.0270	0.0004	171.5	2.5
*2.1	203	232	1.14	4.7	-	0.48	36.655	0.455	0.0533	0.0012	0.0272	0.0003	172.7	2.1
3.1	216	199	0.92	5.5	0.000055	<0.01	34.002	0.415	0.0486	0.0012	0.0295	0.0004	187.1	2.3
4.1	160	170	1.07	3.9	0.000219	0.29	34.983	0.446	0.0520	0.0012	0.0285	0.0004	181.2	2.3
5.1	103	71	0.69	2.6	-	0.51	34.119	0.477	0.0539	0.0015	0.0292	0.0004	185.3	2.6
6.1	233	193	0.83	5.7	0.000045	0.09	34.876	0.418	0.0505	0.0010	0.0286	0.0003	182.1	2.2
7.1	88	65	0.74	2.2	0.000199	0.21	35.000	0.512	0.0514	0.0016	0.0285	0.0004	181.2	2.7
10.1	68	38	0.55	1.6	0.001140	1.27	35.664	0.741	0.0597	0.0021	0.0277	0.0006	176.0	3.7
*11.1	350	568	1.63	7.9	0.000081	<0.01	38.151	0.545	0.0493	0.0009	0.0262	0.0004	166.8	2.4
12.1	161	103	0.64	3.9	-	0.50	35.905	0.453	0.0536	0.0022	0.0277	0.0004	176.2	2.3
13.1	129	130	1.00	3.2	-	0.54	35.154	0.474	0.0540	0.0014	0.0283	0.0004	179.8	2.4
14.1	314	370	1.18	7.7	-	0.10	35.102	0.408	0.0505	0.0009	0.0285	0.0003	180.9	2.1
15.1	240	257	1.07	5.9	-	0.23	35.173	0.424	0.0515	0.0015	0.0284	0.0003	180.3	2.2
16.1	467	573	1.22	11.7	-	<0.01	34.308	0.416	0.0495	0.0008	0.0292	0.0004	185.3	2.2
17.1	302	360	1.19	7.4	0.000074	0.19	35.204	0.474	0.0512	0.0010	0.0284	0.0004	180.2	2.4
							Weighted mean age and 95% c.l. error (excluding points marked *)						**181.5**	**2.3**

Notes: 1. Uncertainties given at the 1σ level, except for the means.

2. Error in FC1 reference zircon calibration was 0.61% & 0.30% for the two analytical sessions. (included in the errors on the means for comparing data from different mounts and methods).

3. f206 % denotes the percentage of ^{206}Pb that is common Pb.

4. Correction for common Pb made using the measured ^{238}U/^{206}Pb and ^{207}Pb/^{206}Pb ratios following Tera and Wasserburg (1972) as outlined in Williams (1998).